

SN 2009E: a faint clone of SN 1987A

A. Pastorello^{1,2,3*}, M. L. Pumo^{1,4}, H. Navasardyan¹, L. Zampieri¹, M. Turatto⁵, J. Sollerman⁶, F. Taddia⁶, E. Kankare⁷, S. Mattila⁷, J. Nicolas⁸, E. Prosperi⁹, A. San Segundo Delgado¹⁰, S. Taubenberger¹¹, T. Boles¹², M. Bachini¹³, S. Benetti¹, F. Bufano⁴, E. Cappellaro¹, A. D. Cason¹⁴, G. Cetrulo¹⁵, M. Ergon⁶, L. Germany¹⁶, A. Harutyunyan¹⁷, S. Howerton¹⁸, G. M. Hurst¹⁹, F. Patat²⁰, M. Stritzinger^{6,21}, L.-G. Strolger²², and W. Wells²³

¹ INAF - Osservatorio Astronomico di Padova, Vicolo dell' Osservatorio 5, I-35122, Padova, Italy

² Astrophysics Research Centre, School of Mathematics and Physics, Queen's University Belfast, Belfast BT7 1NN, United Kingdom

³ Dipartimento di Astronomia, Università di Padova, Vicolo dell'Osservatorio 3, I-35122 Padova, Italy

⁴ INAF - Osservatorio Astrofisico di Catania, via S. Sofia 78, I-95123 Catania, Italy

⁵ INAF - Osservatorio Astronomico di Trieste, Via G. B. Tiepolo 11, I-34143, Trieste, Italy

⁶ Oskar Klein Centre, Department of Astronomy, AlbaNova, Stockholm University, SE-10691, Stockholm, Sweden

⁷ Tuorla Observatory, Department of Physics & Astronomy, University of Turku, Väisäläntie 20, FI-21500, Piikkiö, Finland

⁸ Les Mauruches Observatoire, 364 Chemin de Notre Dame, F-06220, Vallauris, France

⁹ Osservatorio Astronomico di Castelmartini, IAU 160, Via Bartolini 1317, I-51036, Larciano, Pistoia, Italy

¹⁰ Observatorio El Gujio, Onice 21, E-28260, Galapagar, Madrid, Spain

¹¹ Max-Planck-Institut für Astrophysik, Karl-Schwarzschild-Str. 1, D-85741, Garching bei München, Germany

¹² Coddenham Astronomical Observatory, Suffolk, United Kingdom

¹³ Osservatorio Astronomico di Tavolaia, Piazza della Vittoria 41, I-56020 Santa Maria a Monte, Pisa, Italy

¹⁴ private address, 105 Glen Pine Trail, Dawsonville, GA 30543, USA

¹⁵ Osservatorio Astronomico Polse di Cougnes, Zuglio, I-33020 Udine, Italy

¹⁶ Center for Astrophysics and Supercomputing, Swinburne University of Technology, Hawthorn, VIC 3122, Australia

¹⁷ Fundación Galileo Galilei - INAF, Telescopio Nazionale Galileo, 38700 Santa Cruz de la Palma, Tenerife, Spain

¹⁸ private address, 1401 South A, Arkansas City, KS 67005, USA

¹⁹ The Astronomer, 16 Westminster Close, Basingstoke, Hants, RG22 4PP, United Kingdom

²⁰ European Southern Observatory, Karl-Schwarzschild-Str. 2, D-85748, Garching bei München, Germany

²¹ Dark Cosmology Centre, Niels Bohr Institute, University of Copenhagen, Juliane Maries Vej 30, 2100 Copenhagen, Denmark

²² Department of Physics and Astronomy, Western Kentucky University, 1906 College Heights Blvd., Bowling Green, KY 42101-1077, USA

²³ University of Oklahoma, Health Science Center, 1100 N. Lindsay, Oklahoma City, OK 73104, USA

Received XXXXX ; accepted XXXXX

ABSTRACT

Context. 1987A-like events form a rare sub-group of hydrogen-rich core-collapse supernovae that are thought to originate from the explosion of blue supergiant stars. Although SN 1987A is the best known supernova, very few objects of this group have been discovered and, hence, studied.

Aims. In this paper we investigate the properties of SN 2009E, which exploded in a relatively nearby spiral galaxy (NGC 4141) and that is probably the faintest 1987A-like supernova discovered so far. We also attempt to characterize this subgroup of core-collapse supernovae with the help of the literature and present new data for a few additional objects.

Methods. The lack of early-time observations from professional telescopes is compensated by frequent follow-up observations performed by a number of amateur astronomers. This allows us to reconstruct a well-sampled light curve for SN 2009E. Spectroscopic observations which started about 2 months after the supernova explosion, highlight significant differences between SN 2009E and the prototypical SN 1987A. Modelling the data of SN 2009E allows us to constrain the explosion parameters and the properties of the progenitor star, and compare the inferred estimates with those available for the similar SNe 1987A and 1998A.

Results. The light curve of SN 2009E is less luminous than that of SN 1987A and the other members of this class, and the maximum light curve peak is reached at a slightly later epoch than in SN 1987A. Late-time photometric observations suggest that SN 2009E ejected about $0.04 M_{\odot}$ of ^{56}Ni , which is the smallest ^{56}Ni mass in our sample of 1987A-like events. Modelling the observations with a radiation hydrodynamics code, we infer for SN 2009E a kinetic plus thermal energy of about 0.6 foe, an initial radius of $\sim 7 \times 10^{12}$ cm and an ejected mass of $\sim 19 M_{\odot}$. The photospheric spectra show a number of narrow ($v \approx 1800 \text{ km s}^{-1}$) metal lines, with unusually strong Ba II lines. The nebular spectrum displays narrow emission lines of H, Na I, [Ca II] and [O I], with the [O I] feature being relatively strong compared to the [Ca II] doublet. The overall spectroscopic evolution is reminiscent of that of the faint ^{56}Ni -poor type II-plateau supernovae. This suggests that SN 2009E belongs to the low-luminosity, low ^{56}Ni mass, low-energy tail in the distribution of the 1987A-like objects in the same manner as SN 1997D and similar events represent the faint tail in the distribution of physical properties for normal type II-plateau supernovae.

Conclusions.

Key words. stars: supernovae: general – stars: supernovae: individual: SN 2009E – stars: supernovae: individual: SN 1987A – stars: supernovae: individual: SN 1998A

1. Introduction

The explosion of supernova (SN) 1987A in the Large Magellanic Cloud (LMC) was an epic event not only because it was the nearest SN in a period of about 4 centuries, but also because it changed significantly the general understanding of the destiny of massive stars. It was commonly believed that hydrogen-rich (H-rich) type II plateau supernovae (SNe IIP) were generated by the explosion of red supergiant (RSG) stars. However, the unusual photometric evolution of SN 1987A, with a broad light curve peak reached about 3 months after the explosion instead of the classical plateau observed in H-rich SNe, and the direct detection of the progenitor star in pre-explosion images changed this general view and proved that the precursor of this SN in the LMC was instead a blue supergiant (BSG, Arnett et al. 1989 and references therein).

Due to their intrinsic rarity and faint early time luminosity, only very few 1987A-like objects were discovered in the past. Good datasets therefore exist only for a handful of objects (SN 1998A, Woodings et al. 1998, Pastorello et al. 2005; SN 2000cb, Hamuy 2001, Kleiser et al. 2011; SNe 2006V and 2006au, Taddia et al. 2011). In analogy with SN 1987A, some of these objects show broad, delayed light curve peaks in all bands (e.g. SN 1998A), while others (e.g. SN 2000cb and SN 1982F) show 1987A-likeness only in the red bands, while the blue bands display a rather normal type IIP behaviour.

In this context, the discovery of a new sub-luminous SN with a light curve comparable to that of SN 1987A, but with other observed properties (fainter intrinsic luminosity at peak, smaller synthesized ^{56}Ni mass and lower expansion velocity of the ejected material) resembling those of some underluminous type IIP SNe (Turatto et al. 1998, Benetti et al. 2001, Pastorello et al. 2004, 2006, 2009) is even more interesting.

This paper is organized as follows: in Section 2 we give basic information on SN 2009E and its host galaxy, and we present photometric and spectroscopic observations of the SN. In Section 3 we discuss the properties of the progenitor star and the explosion parameters as derived from the characteristics of the nebular spectrum and by modelling the SN observations. In Section 4 we analyse the general properties of the family of SNe similar to SN 1987A, whilst the rate of these events is computed in Section 5. Main conclusions are given in Section 6. Finally, an Appendix has been included to present our sample of 1987A-like events (Appendix A), and to compare the light curves of well monitored objects with those of SN 1987A (Appendix B).

2. Observations of SN 2009E

2.1. The host galaxy

NGC 4141 is classified by HyperLeda¹ as an SBc galaxy, rich in H II regions (NED²). Kewley et al. (2005) estimated the integrated oxygen abundance to be $\log(\text{O}/\text{H}) + 12 = 8.60$ (8.74 in the nucleus). They also estimated a star formation rate (SFR) from the integrated flux of $\text{H}\alpha$, viz. $\sim 0.6 \text{ M}_{\odot} \text{ yr}^{-1}$.

Adopting the recessional velocity corrected for Local Group infall into Virgo quoted by HyperLeda ($v_{\text{vir}} = 2158 \pm 20 \text{ km s}^{-1}$) and a Hubble constant $H_0 = 72 \pm 5 \text{ km s}^{-1} \text{ Mpc}^{-1}$, we obtain a distance of about $29.97 \pm 2.10 \text{ Mpc}$ (i.e. distance modulus $\mu = 32.38 \pm 0.35 \text{ mag}$). The Galactic extinction in the direction of

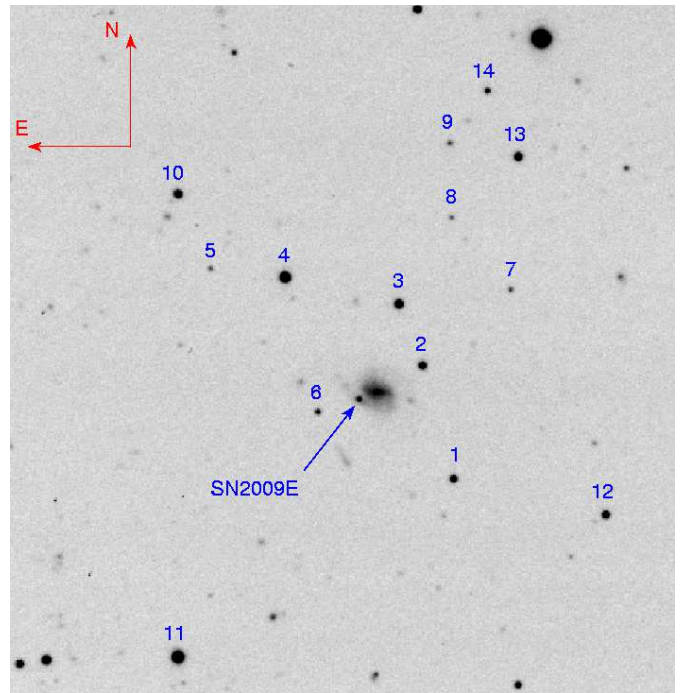


Fig. 1. SN 2009E in NGC 4141. Unfiltered image obtained on April 29, 2009 by J. N. with a 0.28-m f/6.5 reflector equipped with a ST8XME with Kaf1602E CCD. Our sequence of reference stars is marked by numbers. The field of view is about $10' \times 10'$.

NGC 4141 is very low, i.e. $E(B - V) = 0.02 \text{ mag}$ (Schlegel et al. 1998). Narrow interstellar Na I $\lambda\lambda 5889, 5895$ (hereafter Na ID) absorption at the host galaxy rest wavelength is marginally detected in the SN spectra, with an equivalent width (EW) of about 0.12 \AA . Adopting the relation between EW_{NaID} and interstellar extinction from Turatto et al. (2003), we find a host galaxy reddening of $E(B - V) = 0.02 \text{ mag}^3$. The total colour excess in the direction of SN 2009E is therefore $E(B - V) = 0.04 \text{ mag}$.

2.2. The discovery of SN 2009E

SN 2009E was discovered in the spiral galaxy NGC 4141 on January 3rd, 2009, at an unfiltered magnitude of 17.8 (Boles 2009). With the distance and reddening estimated in Section 2.1, the absolute magnitude at the discovery was about -14.7 . The position of SN 2009E is $\alpha = 12^{\text{h}}09^{\text{m}}49^{\text{s}}.56 \pm 0^{\text{s}}.03$, $\delta = +58^{\circ}50'50''.3 \pm 0''.1$ (equinox J2000.0), which is $17''.2$ East and $6''.9$ South of the center of the host galaxy. According to Boles (2009), nothing was visible in pre-explosion images obtained on 2008 February 6th (to limiting magnitude of 19.5). We also found pre-explosion archive g' , R_c and I_c images⁴ obtained on 2008 February 24th at the 0.5-m telescope of the Akeno Observatory/ICRR (Yamanashi, Japan) and no source brighter than $V = 19.5$, $R = 19.6$, $I = 18.8 \text{ mag}$ was visible at the SN position. In this paper, we will adopt January 1.0 UT ($JD=2454832.5$, see Section 2.3) as an indicative epoch for the core-collapse.

Send offprint requests to: A. Pastorello

* email: andrea.pastorello@oapd.inaf.it

¹ <http://leda.univ-lyon1.fr/>

² <http://nedwww.ipac.caltech.edu/index.html>

³ Note, however, that Poznanski et al. (2011) casted doubt on the robustness of the correlation between EW (Na ID) and interstellar extinction as determined from low resolution type Ia SN spectra.

⁴ Images have been downloaded through the SMOKA Data Archive (Baba et al. 2002).

NGC 4141 also hosted the type II SN 2008X (Boles 2008; Madison et al. 2008; Blondin et al. 2008), that exploded 7'6 East and 4'6 North of the nucleus of the galaxy. Interestingly, SN 2008X was another sub-luminous ($M_R \approx -14.9$, Boles 2008) event. The classification spectrum of SN 2008X obtained a few weeks after the explosion showed that it was a type II SN (Blondin et al. 2008), although with rather narrow spectral lines, similar to those observed in SN 2005cs (Pastorello et al. 2006).

Probably the faint apparent magnitude of SN 2009E discouraged astronomers to promptly classify this object. However, later on, Prosperi & Hurst (2009) noted that SN 2009E brightened by 1–1.5 mag during the subsequent two months, and only at about 80 days from the discovery the object was classified by Navasardyan et al. (2009) as a type II SN around the end of the H recombination phase. SN 2009E appeared to show some similarity with the peculiar SN 1987A, especially in the late-time light curve brightening and the unusual strength of the Ba II P-Cygni lines. The most obvious differences were in the lower luminosity and the much narrower spectral features.

2.3. Light Curves

Whilst professional astronomers initially missed to follow this transient object, amateur astronomers monitored SN 2009E extensively, and it is thanks to their efforts that we can now recover information on the early flux evolution. Most images collected during the period January 2009 to May 2009 were from amateur observations. Since the end of March, we started multiband photometric and spectroscopic follow-up observations with larger, professional telescopes. All photometric data were reduced with standard techniques in IRAF⁵. Images were first overscan, bias and flat-field corrected. Then, photometric measurements of filtered images were performed using a PSF-fitting technique because suitable template images were not available. However, since the SN location was quite peripheral in the galaxy arm, its luminosity largely exceeded that of the surroundings, except at very late epochs when the SN became weak. We estimated the uncertainty due to the non-flat background by placing in all images several artificial stars close to the SN location. The adopted errors were the r.m.s. of the recovered artificial star PSF magnitudes. Multi-band zero-points for the different nights were computed through observations of standard stellar fields (Landolt 1992) obtained during the same nights as the SN observations. The SN magnitudes were finally fine tuned with reference to a sequence of stars in the field of NGC 4141 (see Figure 1), calibrated by averaging magnitudes measured in selected photometric nights. The magnitudes of the local sequence stars are shown in Table 1, while the final SN magnitudes are reported in Table 2.

Since a number of unfiltered pre-explosion images of NGC 4141 were available, magnitude measurements on the amateurs' images were performed with the PSF-fitting technique after subtraction of the best seeing host galaxy template image. In this way we minimized the contamination of the background sources near the SN location. The subsequent photometric calibration was performed with the prescriptions discussed in Pastorello et al. (2008). Since the detectors used by amateur astronomers in their follow-up campaign of SN 2009E have quantum efficiencies preferentially peaking at $\sim 5700\text{--}6500\text{ \AA}$, unfiltered

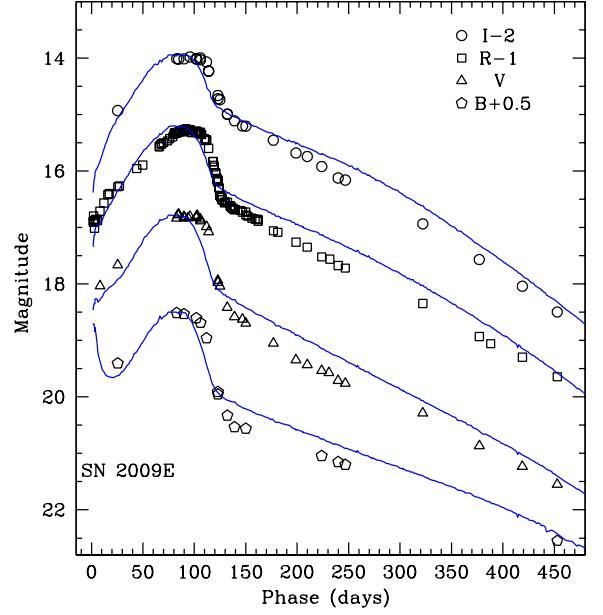


Fig. 2. *B*, *V*, *R* and *I*-band light curves of SN 2009E compared with those of SN 1987A (solid blue line; Menzies et al. 1987; Catchpole et al. 1987, 1988, 1989; Whitelock et al. 1988, 1989), shifted arbitrarily in magnitude to match the peak magnitudes of SN 2009E.

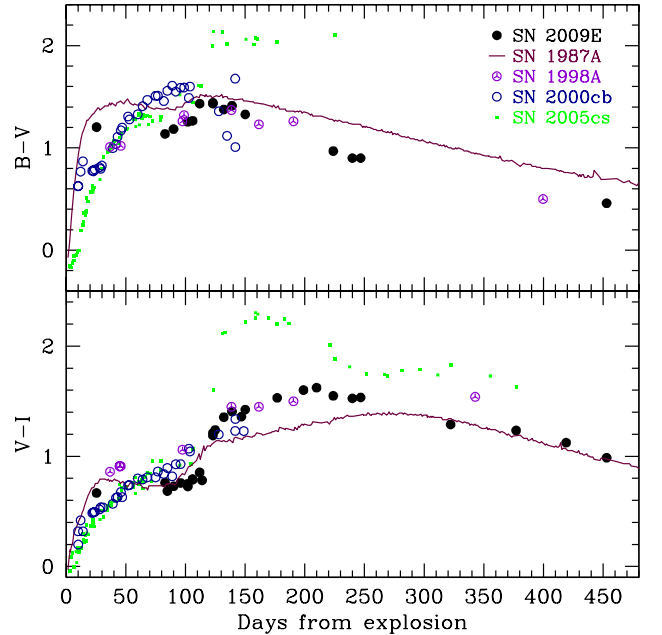


Fig. 3. *B - V* (top) and *V - I* (bottom) colour curves of SN 2009E compared with those of a subsample of SN 1987A-like events with multi-colour photometric coverage: SNe 1987A (Menzies et al. 1987; Catchpole et al. 1987, 1988, 1989; Whitelock et al. 1988, 1989), 1998A (Pastorello et al. 2005), and 2000cb (Hamuy 2001). The colour curves of the sub-luminous type IIP SN 2005cs (Tsvetkov et al. 2006; Pastorello et al. 2009) is also shown for comparison.

⁵ IRAF is distributed by the National Optical Astronomy Observatories, which are operated by the Association of Universities for Research in Astronomy, Inc., under cooperative agreement with the National Science Foundation.

Table 1. Magnitudes of reference stars in the SN field, calibrated on several photometric nights. The root mean square of the average magnitudes are reported in brackets.

Star	<i>U</i>	<i>B</i>	<i>V</i>	<i>R</i>	<i>I</i>
1	18.86 (0.03)	17.59 (0.02)	16.52 (0.02)	15.74 (0.01)	15.18 (0.01)
2	17.47 (0.02)	16.88 (0.01)	16.11 (0.01)	15.60 (0.01)	15.20 (0.01)
3	15.85 (0.04)	15.87 (0.01)	15.35 (0.01)	15.01 (0.01)	14.69 (0.01)
4	18.07 (0.03)	16.89 (0.01)	15.41 (0.02)	—	—
5	18.81 (0.03)	18.73 (0.01)	18.05 (0.02)	17.62 (0.01)	17.19 (0.02)
6	17.75 (0.03)	17.85 (0.01)	17.26 (0.01)	16.83 (0.01)	16.43 (0.01)
7	20.76 (0.05)	19.33 (0.02)	18.17 (0.01)	17.31 (0.01)	16.56 (0.02)
8	18.97 (0.05)	18.91 (0.02)	18.23 (0.01)	17.78 (0.01)	17.37 (0.01)
9	—	19.90 (0.02)	18.46 (0.02)	17.47 (0.01)	16.58 (0.02)
10	—	16.32 (0.01)	15.70 (0.02)	15.31 (0.02)	14.94 (0.01)
11	—	14.45 (0.02)	13.73 (0.03)	13.15 (0.04)	12.83 (0.01)
12	—	16.43 (0.03)	15.86 (0.03)	15.48 (0.01)	15.11 (0.02)
13	16.63 (0.06)	16.40 (0.01)	15.67 (0.02)	15.22 (0.01)	14.78 (0.02)
14	—	19.86 (0.06)	18.27 (0.10)	—	—

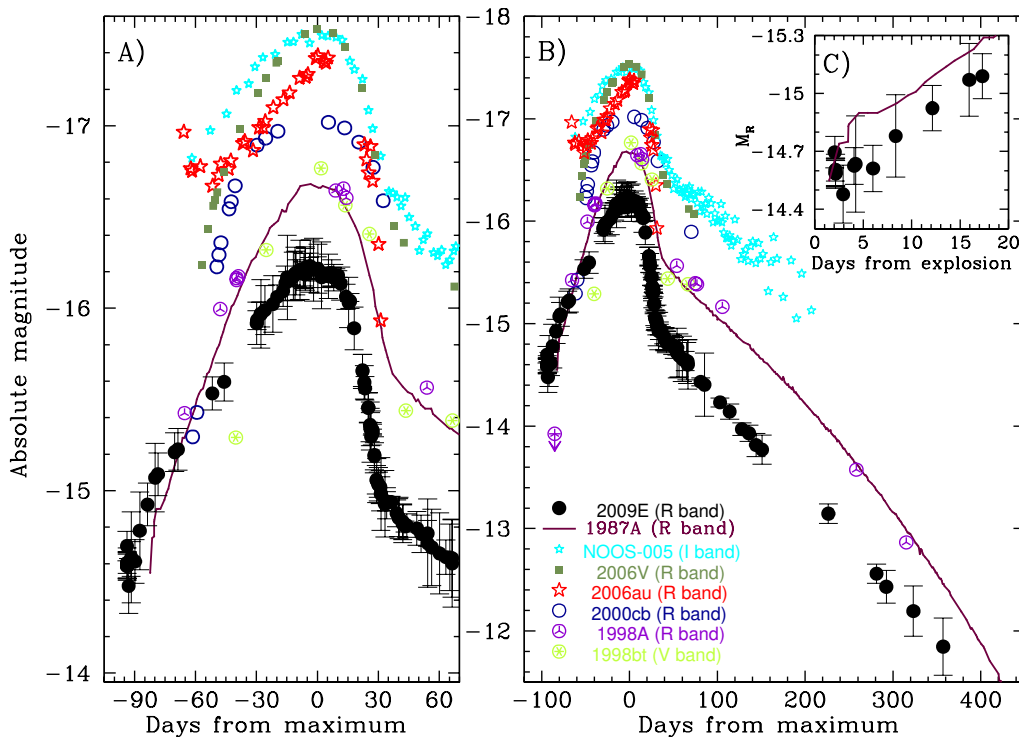


Fig. 4. *R*-band absolute light curve of SN 2009E compared with the absolute light curves of a number of SN 1987A-like events: NOOS-005 (*I* band, OGLE collaboration), SNe 2006V, 2006au, 1998bt (*V* band, L. Germany, private communication, see also Germany 1998), 2000cb, 1998A and the prototype 1987A. Panel A: detail on the broad light curve peak. Panel B: the full light curve evolution. Panel C: blow-up of the very early-time light curves of SNe 2009E and 1987A, soon after shock break-out.

tered magnitudes were scaled to match the *R*-band photometry. The SN magnitude errors accounted for the uncertainties in this conversion. The final *R*-band-calibrated magnitudes are reported in Table 2, marked with an asterisk. The *B*, *V*, *R*, *I* light curves of SN 2009E, compared with those of SN 1987A, are shown in Figure 2.

In Figure 3 we compare the *B* – *V* and *V* – *I* colour curves of SN 2009E with those of a subsample of 1987A-like events and with the sub-luminous type IIP SN 2005cs. The colour curves of SN 2009E are remarkably similar to those of SN 1987A at all phases. The colour estimates at phase ~ 25 days ($B - V \approx 1.2$ and $V - I \approx 0.7$ mag) suggest that, in analogy with SN 1987A, SN

2009E became red in a time scale that is shorter than for classical SNe IIP (about 1 month for SN 2009E, while ~ 2 months for type IIP SNe). Between day 30 and day 110, during the recombination phase, the colours remain almost constant. Then, with the post-peak luminosity decline, the SN becomes redder again, reaching $B - V \approx 1.4$ between 110 and 140 days after explosion (this is remarkably similar to the $B - V$ colour observed in SN 1987A). The $V - I$ colour, instead, peaks at about 200 days ($V - I \approx 1.6$ mag), which is a bit earlier than observed for SN 1987A ($V - I \approx 1.4$ mag between 230 and 310 days). Subsequently, the colours turn back to the blue again.

Table 2. Calibrated U , B , V , R , I band magnitudes of SN 2009E. The numbers in column 8 identify the different instrumental configurations. Unfiltered observations rescaled to R-band magnitudes are marked with the symbol “★”. The “★★” symbol marks two epochs in which both filtered (V or I band) and unfiltered observations were collected. The symbol “‡” marks a g' -band observation converted into Johnson-Bessell V band.

Date	JD	U	B	V	R	I	Instrument
Feb06 2008	2454502.5	–	–	–	>19.5	–	1★
Feb24 2008	2454521.22	–	–	>19.5‡	>19.6	>18.9	2
Jan03 2009	2454834.56	–	–	–	17.79 (0.08)	–	1★
Jan03 2009	2454834.63	–	–	–	17.89 (0.06)	–	1★
Jan03 2009	2454834.63	–	–	–	17.89 (0.08)	–	1★
Jan03 2009	2454834.64	–	–	–	17.90 (0.08)	–	1★
Jan03 2009	2454834.64	–	–	–	17.91 (0.07)	–	1★
Jan03 2009	2454834.65	–	–	–	17.90 (0.08)	–	1★
Jan03 2009	2454835.42	–	–	–	18.01 (0.15)	–	1★
Jan05 2009	2454836.56	–	–	–	17.87 (0.10)	–	3★
Jan05 2009	2454836.71	–	–	–	17.86 (0.25)	–	4★
Jan07 2009	2454838.51	–	–	–	17.88 (0.12)	–	5★
Jan09 2009	2454840.84	–	–	18.04 (0.33)	17.71 (0.21)	–	6
Jan13 2009	2454844.63	–	–	–	17.57 (0.12)	–	4★
Jan16 2009	2454848.44	–	–	–	17.42 (0.19)	–	6★
Jan18 2009	2454849.80	–	–	–	17.40 (0.12)	–	7★
Jan26 2009	2454858.01	>20.35	18.91 (0.29)	17.66 (0.13)	17.28 (0.11)	16.93 (0.07)	8
Jan28 2009	2454859.64	–	–	–	17.26 (0.11)	–	9★
Feb14 2009	2454876.56	–	–	–	16.96 (0.09)	–	10★
Feb19 2009	2454882.39	–	–	–	16.89 (0.10)	–	11★
Mar07 2009	2454898.48	–	–	–	16.57 (0.12)	–	10★
Mar08 2009	2454898.55	–	–	–	16.56 (0.05)	–	6★
Mar09 2009	2454900.42	–	–	–	16.52 (0.07)	–	6★
Mar09 2009	2454900.46	–	–	–	16.52 (0.19)	–	12★
Mar11 2009	2454902.50	–	–	–	16.50 (0.13)	–	10★
Mar15 2009	2454906.44	–	–	–	16.47 (0.16)	–	10★
Mar18 2009	2454908.58	–	–	–	16.43 (0.07)	–	13★
Mar20 2009	2454911.49	–	–	–	16.40 (0.08)	–	10★
Mar22 2009	2454912.57	–	–	–	16.35 (0.09)	–	9★
Mar23 2009	2454913.50	–	–	–	16.32 (0.23)	–	14★
Mar23 2009	2454913.67	–	–	–	16.33 (0.04)	–	15★
Mar24 2009	2454915.41	–	18.02 (0.10)	16.84 (0.03)	16.33 (0.03)	16.01 (0.02)	16
Mar25 2009	2454916.42	–	–	–	16.32 (0.13)	–	10★
Mar25 2009	2454916.46	–	–	16.78 (0.05)	–	–	17
Mar26 2009	2454917.33	–	–	16.77 (0.14)	16.30 (0.15)	16.02 (0.17)	17★
Mar27 2009	2454917.73	–	–	–	16.30 (0.12)	–	15★
Mar27 2009	2454918.38	–	–	–	16.30 (0.07)	–	3★
Mar29 2009	2454919.75	–	–	–	16.28 (0.16)	–	15★
Mar30 2009	2454921.42	–	–	–	16.30 (0.07)	–	3★
Mar31 2009	2454921.70	–	–	–	16.29 (0.10)	–	15★
Mar31 2009	2454922.36	–	–	–	16.27 (0.12)	–	17★
Mar31 2009	2454922.43	–	–	–	16.27 (0.11)	–	10★
Mar31 2009	2454922.49	–	18.03 (0.02)	16.81 (0.01)	16.31 (0.01)	16.02 (0.01)	18
Apr01 2009	2454923.34	–	–	16.83 (0.04)	16.29 (0.04)	–	19
Apr02 2009	2454924.39	–	–	–	16.27 (0.06)	–	3★
Apr02 2009	2454924.44	–	–	–	16.26 (0.07)	–	17★
Apr03 2009	2454924.75	–	–	–	16.26 (0.14)	–	15★
Apr04 2009	2454926.42	–	–	16.83 (0.08)	–	–	19
Apr04 2009	2454926.45	–	–	–	16.28 (0.17)	–	10★
Apr06 2009	2454928.33	–	–	16.80 (0.06)	–	15.98 (0.03)	19
Apr06 2009	2454928.34	–	–	–	16.28 (0.07)	–	3★
Apr07 2009	2454928.61	–	–	–	16.27 (0.13)	–	9★
Apr08 2009	2454930.32	–	–	–	16.31 (0.18)	–	17★
Apr08 2009	2454930.42	–	–	–	16.32 (0.06)	–	10★
Apr12 2009	2454933.79	–	–	–	16.32 (0.12)	–	15★
Apr12 2009	2454934.39	–	–	16.82 (0.04)	–	16.01 (0.03)	19

Table 2. continued.

Date	<i>JD</i>	<i>U</i>	<i>B</i>	<i>V</i>	<i>R</i>	<i>I</i>	Instrument
Apr12 2009	2454934.46	19.53 (0.11)	18.10 (0.02)	16.81 (0.01)	16.300 (0.01)	16.02 (0.02)	18
Apr13 2009	2454935.36	—	—	16.79 (0.07)	16.300 (0.08)	—	6★★
Apr13 2009	2454935.40	—	—	—	16.32 (0.05)	—	3★
Apr14 2009	2454936.37	—	—	—	16.32 (0.07)	—	17★
Apr15 2009	2454937.34	—	—	—	16.33 (0.05)	—	17★
Apr16 2009	2454938.41	—	—	16.85 (0.03)	16.31 (0.03)	16.00 (0.02)	20
Apr17 2009	2454938.53	—	18.19 (0.02)	16.88 (0.01)	16.33 (0.01)	16.03 (0.01)	18
Apr18 2009	2454939.76	—	—	—	16.36 (0.09)	—	15★
Apr20 2009	2454942.39	—	—	—	16.43 (0.07)	—	3★
Apr22 2009	2454943.74	—	—	—	16.46 (0.14)	—	15★
Apr22 2009	2454944.32	—	—	—	16.45 (0.14)	—	6★
Apr22 2009	2454944.38	—	18.46 (0.35)	16.99 (0.10)	16.45 (0.04)	16.07 (0.08)	6
Apr24 2009	2454946.40	—	—	17.08 (0.07)	16.60 (0.12)	16.23 (0.04)	6★★
Apr24 2009	2454946.45	—	—	—	—	16.23 (0.03)	6
Apr29 2009	2454950.56	—	—	—	16.83 (0.09)	—	9★
Apr29 2009	2454950.58	—	—	—	16.84 (0.09)	—	13★
Apr29 2009	2454951.45	—	—	—	16.90 (0.09)	—	3★
Apr30 2009	2454951.74	—	—	—	16.93 (0.06)	—	15★
May01 2009	2454953.37	—	—	—	17.04 (0.08)	—	10★
May01 2009	2454953.42	—	—	—	17.03 (0.08)	—	6★
May02 2009	2454954.34	—	—	—	17.13 (0.09)	—	3★
May02 2009	2454954.37	—	—	—	17.14 (0.13)	—	10★
May02 2009	2454954.48	—	—	—	17.15 (0.09)	—	17★
May03 2009	2454954.78	—	—	—	17.19 (0.14)	—	15★
May03 2009	2454955.34	—	—	—	17.18 (0.06)	—	6★
May03 2009	2454955.45	—	19.41 (0.13)	17.94 (0.06)	17.16 (0.03)	16.66 (0.02)	20
May04 2009	2454955.53	20.85 (0.16)	19.46 (0.03)	17.97 (0.01)	17.17 (0.01)	16.72 (0.01)	18
May04 2009	2454956.39	—	—	—	17.29 (0.10)	—	3★
May04 2009	2454956.39	—	—	—	17.30 (0.07)	—	10★
May05 2009	2454957.38	—	—	—	17.43 (0.08)	—	10★
May05 2009	2454957.42	—	—	18.04 (0.13)	—	16.74 (0.06)	6
May06 2009	2454957.60	—	—	—	17.44 (0.12)	—	9★
May06 2009	2454958.36	—	—	—	17.46 (0.07)	—	10★
May06 2009	2454958.40	—	—	—	17.46 (0.09)	—	3★
May07 2009	2454959.35	—	—	—	17.47 (0.09)	—	6★
May08 2009	2454959.54	—	—	—	17.51 (0.09)	—	17★
May08 2009	2454959.64	—	—	—	17.51 (0.20)	—	15★
May10 2009	2454961.56	—	—	—	17.56 (0.18)	—	6★
May10 2009	2454962.37	—	—	—	17.56 (0.09)	—	17★
May10 2009	2454962.39	—	—	—	17.55 (0.05)	—	3★
May13 2009	2454964.66	>20.23	19.83 (0.13)	18.42 (0.06)	17.55 (0.03)	16.99 (0.03)	21
May15 2009	2454967.36	—	—	—	17.61 (0.07)	—	10★
May16 2009	2454968.36	—	—	—	17.64 (0.11)	—	3★
May17 2009	2454968.57	—	—	—	17.64 (0.11)	—	7★
May18 2009	2454970.35	—	—	—	17.66 (0.10)	—	6★
May18 2009	2454970.36	—	—	—	17.67 (0.10)	—	10★
May20 2009	2454971.52	>21.08	20.04 (0.09)	18.58 (0.03)	17.69 (0.03)	17.11 (0.02)	21
May20 2009	2454972.35	—	—	—	17.68 (0.06)	—	6★
May25 2009	2454977.34	—	—	—	17.70 (0.09)	—	17★
May27 2009	2454979.37	—	—	18.63 (0.22)	17.73 (0.10)	17.20 (0.14)	16
May31 2009	2454982.59	—	20.06 (0.29)	18.69 (0.12)	17.72 (0.07)	17.21 (0.07)	20
May31 2009	2454982.65	—	—	—	17.78 (0.24)	—	13★
Jun02 2009	2454984.66	—	—	—	17.80 (0.21)	—	15★
Jun06 2009	2454988.50	—	—	—	17.83 (0.22)	—	9★
Jun09 2009	2454991.65	—	—	—	17.86 (0.09)	—	13★
Jun11 2009	2454993.58	—	—	—	17.86 (0.18)	—	9★
Jun12 2009	2454994.62	—	—	—	17.86 (0.21)	—	9★
Jun12 2009	2454994.72	—	—	—	17.89 (0.24)	—	15★
Jun26 2009	2455009.38	—	—	19.05 (0.11)	18.06 (0.04)	17.45 (0.03)	20
Jul01 2009	2455013.67	—	—	—	18.09 (0.31)	—	15★

Table 2. continued.

Date	<i>JD</i>	<i>U</i>	<i>B</i>	<i>V</i>	<i>R</i>	<i>I</i>	Instrument
Jul18 2009	2455031.39	–	–	19.35 (0.10)	18.26 (0.04)	17.68 (0.04)	20
Jul29 2009	2455042.36	–	–	19.43 (0.11)	18.35 (0.07)	17.74 (0.05)	16
Aug12 2009	2455056.35	–	20.54 (0.20)	19.54 (0.15)	18.52 (0.06)	17.92 (0.05)	20
Aug19 2009	2455063.37	–	–	19.57 (0.12)	–	–	16
Aug20 2009	2455064.32	–	–	–	18.56 (0.08)	–	16
Aug28 2009	2455072.34	–	20.65 (0.32)	19.71 (0.16)	18.67 (0.11)	18.12 (0.08)	20
Sep04 2009	2455079.34	–	20.70 (0.21)	19.76 (0.15)	18.72 (0.14)	18.16 (0.13)	20
Nov19 2009	2455154.69	–	–	20.29 (0.27)	19.35 (0.10)	18.94 (0.04)	20
Jan13 2010	2455209.60	–	–	20.87 (0.12)	19.93 (0.09)	19.57 (0.08)	18
Jan24 2010	2455220.69	–	–	–	20.06 (0.16)	–	18★
Feb24 2010	2455251.50	–	–	21.23 (0.37)	20.30 (0.25)	20.04 (0.23)	18
Mar29 2010	2455285.43	–	22.05 (0.45)	21.55 (0.18)	20.64 (0.28)	20.50 (0.12)	21

- 1 = 0.36-m C14 reflector + Apogee AP7 CCD camera (Obs. T. Boles, Coddendham Observatory, Suffolk, UK);
2 = 0.50-m Telescope + Apogee U6 CCD camera (Obs. M. Yoshida, Akeno Observatory/ICRR, Yamanashi, Japan);
3 = 0.28-m C11 reflector + SBIG ST-8XME Kaf1602E CCD camera (Obs. J. Nicolas, Vallauris, France);
4 = 0.28-m C11 reflector + SBIG ST-8XME Kaf1602E CCD camera (Obs. J. M. Llapasset, Perpignan, France);
5 = 0.36-m C14 reflector + Apogee AP7 CCD Camera (Obs. O. Trondal, Groruddalen, Oslo, Norway);
6 = 0.36m Meade LX200 Telescope + SBIG ST-9XE CCD camera (Obs. E. Prosperi, Osservatorio Astronomico di Castelmartini, Larciano, Pistoia, Italy);
7 = 0.3-m Takahashi Mewlon 300 + SBIG ST-8E NABG camera (obs. W. Wells, Gras-002, New Mexico, USA);
8 = 2.0-m Faulkes Telescope North + EM01 (Faulkes Telescope Archive - Las Cumbres Observatory, Mt. Haleakala, Hawaii Islands, USA);
9 = 0.35-m Bradford Robotic Telescope + FLI MaxCam CM2-1 camera with E2V CCD47-10 (Obs. G. Hurst, Tenerife Observatory, Canary Islands, Spain);
10 = 0.20-m C8 reflector + SBIG ST-9 Kaf0261 CCD camera (obs. A. San Segundo Delgado, Observatorio El Guijo, Galapagar, Madrid, Spain);
11 = 0.25-m Newton Telescope + Meade DSI Pro camera with Sony EXView HAD CCD (Obs. R. Mancini and F. Briganti, Associazione Astronomica Isaac Newton, Stazione di Gavena, Cerreto Guidi, Italy);
12 = 0.40-m reflector + DTA camera with Kodak Kaf0260 CCD (G. Iacopini, Osservatorio della Tavolaia, Associazione Astronomica Isaac Newton, Santa Maria a Monte, Pisa, Italy);
13 = 0.25-m Meade 10" LX200 Telescope + SBIG ST-8XME Kaf1602E CCD camera (Obs. A. D. Cason, Dawsonville, Georgia, USA);
14 = 0.5-m Newton-Cassegrain Telescope + Hi-Sis 44 CCD camera (Obs. A. Dimai, Osservatorio di Col Drusciè, Cortina, Italy);
15 = 0.3-m Takahashi Mewlon 300 + FLI IMG1024 DM camera (obs. S. Howerton, Gras-001, New Mexico, USA);
16 = 1.82-m Copernico Telescope + AFOSC (INAF - Osservatorio Astronomico di Asiago, Mt. Ekar, Asiago, Italy);
17 = 0.30-m Meade LX200 Telescope + SBIG ST-10XME CCD camera (Obs. E. Prosperi, Skyline Remote Facility, Osservatorio B40 Skyline, Pedata, Catania, Italy);
18 = 2.56-m Nordic Optical Telescope + ALFOSC (La Palma, Canary Islands, Spain);
19 = 0.7-m Ritchey-Chrétien Telescope + Apogee Alta U9000 camera with Kodak Kaf-09000 CCD (Obs. A. Englaro, I. Bano and G. Cetrulo, Osservatorio Astronomico di Polse di Cougnes, Zuglio, Udine, Italy);
20 = 2.2-m Calar Alto Telescope + CAFOS (German-Spanish Astronomical Center, Andalucía, Spain);
21 = 3.58-m Telescopio Nazionale Galileo + Dolores (Fundación Galileo Galilei - INAF, La Palma, Canary Islands, Spain).

The *R*-band absolute light curve of SN 2009E is shown in Figure 4, together with those of a number of other type II SNe with a broad, delayed light curve peak, similar to that observed for SN 1987A. In analogy with the early discovery of SN 1987A (Arnett et al. 1989), also SN 2009E was likely caught soon after the core-collapse. Marginal evidence of the initial sharp peak due to the shock breakout is possibly visible (Figure 4, panel C), although the large error bars of the unfiltered amateur images make this finding rather uncertain.

Nevertheless, we can constrain the explosion epoch of SN 2009E with a small uncertainty through a comparison with the early photometric evolution of SN 1987A. Hereafter we will adopt $JD=2454832.5^{+2}_{-5}$ as the best estimate for the core-collapse epoch of SN 2009E. The distances and reddenings used for our sample of 1987A-like events shown in Figure 4 are listed in Tables 4 and 5. SN 2009E is the faintest SN in this sample at all the epochs. In particular, its peak magnitude $M_R \sim -16.2$ is about 0.4 mag fainter than that of SN 1987A and its ^{56}Ni mass, as derived from the luminosity of the radioactive tail relative to that of SN 1987A, is $0.040^{+0.015}_{-0.011} M_{\odot}$, the lowest among the objects in our sample.

Another remarkable property of SN 2009E is that its *R*-band light curve peaks at about +96d after core-collapse, significantly later than SN 1987A ($\sim +84$ days). This suggests different ejecta parameters for SN 2009E (e.g. smaller initial radius, lower expansion velocity or a more massive envelope, see Section 3.2). Interestingly, fainter SNe in our sample seem to reach peak magnitude later than the more luminous ones (see also Appendix B).

2.4. Spectra

As mentioned above, the spectroscopic classification of SN 2009E was performed about 80 days after the SN discovery. To our knowledge, no spectra exist to witness the early time evolution of this object. After the SN classification, we started a regular spectroscopic monitoring covering the SN evolution from near maximum light to the nebular phase. Spectra have been reduced in the IRAF environment using standard prescriptions. After the optimal extraction, the SN spectra were wavelength calibrated using arc lamp spectra and then flux calibrated using flux standard stars observed in the same nights as the SN. A final check with photometry was performed in order to fine tune the flux calibration of the spectra, with a remaining uncertainty in the flux calibration of less than 10%. Basic information on the spectra collected for SN 2009E is listed in Table 3, while the spectral sequence until August 15, 2009 is shown in Figure 5.

Since the earliest spectrum was obtained about 83 days after the core-collapse, the continuum is quite red, indicative of relatively low temperatures ($T_{bb} \approx 6000$ K). All the photospheric spectra show a clear flux deficit at the blue wavelengths (below 4500 Å) that is due to line blanketing from increasingly strong metal lines. These spectra are rich in narrow P-Cygni lines indicating remarkably low velocity of the expanding ejecta. From the position of the minima of the Sc II $\lambda 6245$ and $\lambda 5527$ lines, we measured $v_{ph} \approx 1600$ km s $^{-1}$ in our earliest spectrum and about 1000 km s $^{-1}$ at the end of the photospheric phase (Figure 6). In the same period, the velocity of the unblended Ba II $\lambda 6142$ line declines from 2200 km s $^{-1}$ to 1850 km s $^{-1}$.

In Figure 7, a late time photospheric spectrum of SN 2009E (phase about 3 months after explosion) is compared with spectra of SN 1987A and the 1987A-like event SN 1998A (Pastorello et al. 2005.; see also Figure 7, top panel), and with spectra of faint SNe IIP (Turatto et al. 1998; Benetti et al. 2001;

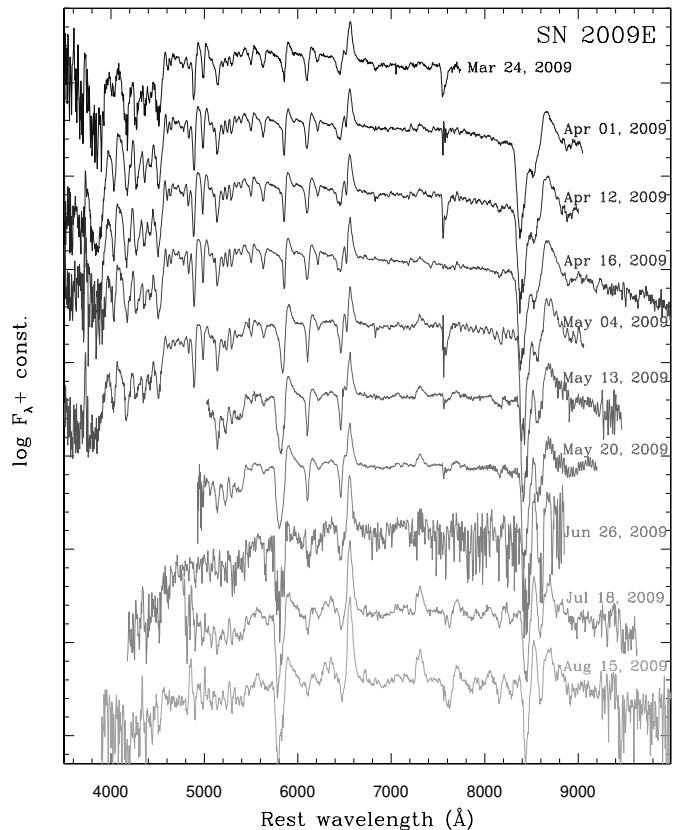


Fig. 5. Spectral sequence for SN 2009E, starting from about 80 days after core-collapse.

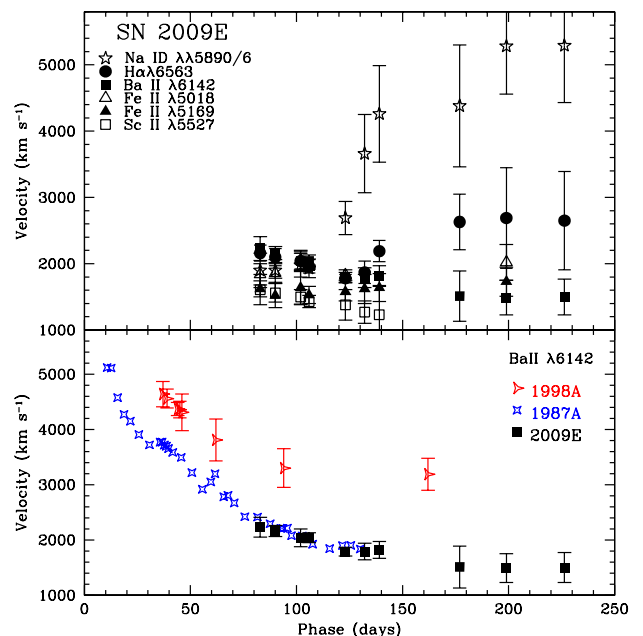


Fig. 6. Top: Evolution of the expansion velocities for the principal lines in the spectra of SN 2009E. Bottom: comparison of the velocities derived for the Ba II $\lambda 6142$ line in SNe 2009E, 1987A and 1998A.

Table 3. Spectroscopic observations of SN 2009E.

Date	Average JD	Phase*	Instrumental configuration	Exposure (s)	Resolution (\AA) [•]	Range (\AA)
Mar24, 2009	2454915.40	+82.9	Ekar1.82m+AFOSC+gr4	3600	24	3490–7790
Mar25, 2009 [‡]	2454915.54	+83.0	Asiago1.22m+B&C+g600	3600	6.1	5090–7500
Apr01, 2009	2454922.52	+90.0	NOT+ALFOSC+gr4	1200	13	3360–9100
Apr12, 2009	2454934.48	+102.0	NOT+ALFOSC+gr4	1200	16	3230–9060
Apr16, 2009	2454938.42	+105.9	CAHA2.2m+CAFOS+g200	1792	9.5	3700–10670
May04, 2009	2454955.57	+123.1	NOT+ALFOSC+gr4	2700	13	3350–9120
May13, 2009	2454964.62	+132.1	TNG+LRS+LRR	3600	12	5050–9520
May20, 2009	2454971.55	+139.1	TNG+LRS+LRR	3600	12	4960–9560
Jun26, 2009 [‡]	2455009.42	+176.9	CAHA2.2m+CAFOS+g200	2×2400	9.5	4100–9100
Jul18, 2009	2455031.44	+198.9	CAHA2.2m+CAFOS+g200+GG495	2×3600	13	4800–9690
Aug15, 2009 [†]	2455058.84	+226.3	CAHA2.2m+CAFOS+g200	2×3600	12	3880–10670
Jan22, 2010	2455218.64	+386.1	NOT+ALFOSC+gr5	3×1200	14	5000–10000
Jan24, 2010	2455220.70	+388.2	NOT+ALFOSC+gr4	3×1200	12	3550–9080

* Days from explosion ($JD=2454832.5$); [•] As estimated from the full width at half maximum of isolated night sky lines. [‡] Poor signal-to-noise spectrum; [†] Weighted average of 2 spectra obtained on August 14th and 15th.

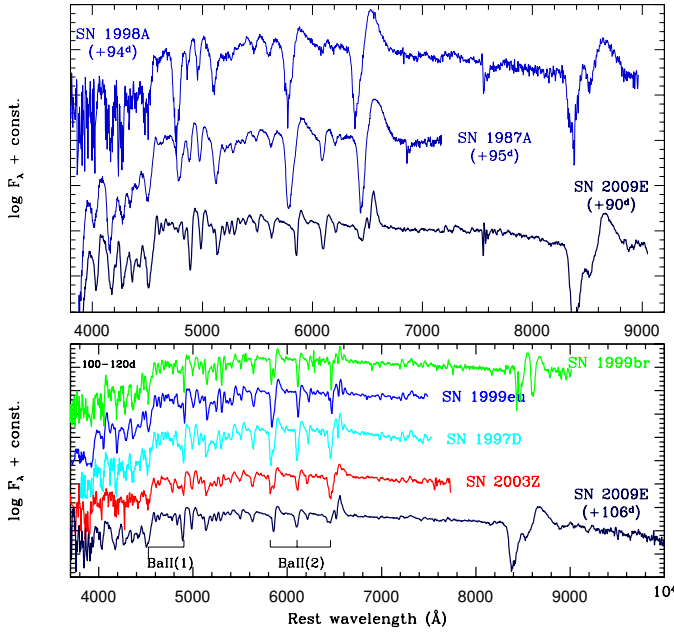


Fig. 7. Top: A spectrum of SN 2009E obtained on Apr 1st, 2009 is compared with spectra of SNe 1998A (Pastorello et al. 2005) and 1987A (Pun et al. 1995) at a similar phase. Bottom: a post-maximum spectrum of SN 2009E (Apr 16th, 2009) is compared with spectra of underluminous type IIP SNe obtained around the end of the plateau phase (Turatto et al. 1998; Pastorello et al. 2004).

Pastorello et al. 2004, 2009, see Figure 7, bottom panel). While the strong Ba II lines are a common feature both for the spectra of SN 1987A and under-luminous, ^{56}Ni -poor type IIP SNe, the narrowness of the spectral lines in SN 2009E is more reminiscent of 1997D-like events (Turatto et al. 1998; Pastorello et al. 2004).

Together with quite a weak $H\alpha$, we clearly identify prominent lines of Na I D, Ca II, O I, Fe II, Ti II, Sc II and Cr II [see Pastorello et al. (2006) for a detailed line identification for underluminous SNe IIP during the photospheric phase, and Benetti et al. (2001) for the nebular phase]. The Ba II lines (multiplet 2) are among the strongest spectral features. This is

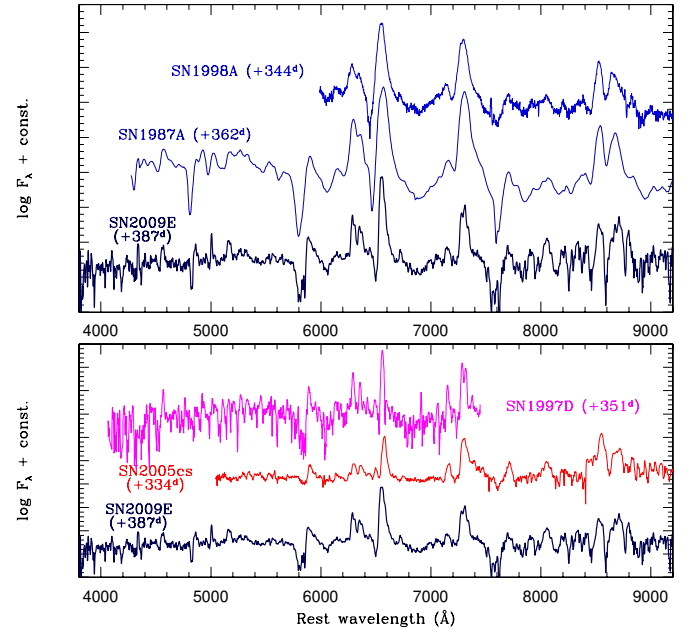


Fig. 8. Top: A nebular spectrum of SN 2009E is compared with spectra of SNe 1998A (Pastorello et al. 2005) and 1987A (Pun et al. 1995) at a similar phase (~ 1 year). The nebular spectrum of SN 2009E was obtained averaging spectra of 2010 Jan 22nd and 24th. Bottom: the nebular spectrum of SN 2009E is compared with spectra of underluminous type IIP SNe obtained about 1 year after core-collapse (Benetti et al. 2001; Pastorello et al. 2009).

a common characteristic of both SN 1987A (Williams 1987; Mazzali et al. 1992; Mazzali & Chugai 1995) and faint SNe IIP (Pastorello et al. 2004). The presence of prominent Ba II lines in the photospheric spectra of SN 1987A was interpreted by Tsujimoto & Shigeyama (2001) as a signature of an over-abundance of Ba in the outer layers of the SN ⁶. However, the presence of prominent Ba II features in underluminous SNe IIP

⁶ Note that Utrobin & Chugai (2005) favoured time-dependent ionization effects to explain the presence of prominent Ba II lines in photospheric spectra of SN 1987A.

can also be explained invoking temperature effects. The evolution of Na ID is puzzling. The absorption component becomes broader with time (see Figure 5 for the evolution of this spectral feature from 2009 April 16 to May 13). A similar behaviour, although less extreme, is observed also for H α . This effect is probably due to line blending, with the Ba II λ 5854 and λ 6497 lines (and possibly of other metal features) having an increasing strength relative to Na ID and H α respectively. The evolution of the expansion velocities, as deduced from the minima of the P-Cygni of H α , Na I, Ba II, Fe II and Sc II, is shown in Figure 6. Metal lines show a monotonic decline and velocities at the end of the plateau phase (1200–1800 km s⁻¹) that are only marginally higher than those observed in sub-luminous type IIP SNe (800–1200 km s⁻¹, see e.g. Turatto et al. 1998; Pastorello et al. 2004, 2009), whilst H α and Na ID display an opposite trend. Since May (around 4 months past explosion, Figure 5), the classical nebular doublets of [Ca II] λ 7291–7323 and [O I] λ 6300–6364 become visible, and increase in strength with time.

A late time spectrum of SN 2009E was obtained at the Nordic Optical Telescope (NOT) about 1 year after explosion (see Figure 8). Although the transition toward a purely nebular appearance is not complete (e.g. broad P-Cygni features of Na ID, O I λ 7774 and Ca II NIR are still visible), the spectrum is clearly dominated by prominent H α in emission, [O I] λ 6300,6364 and [Ca II] λ 7291,7323. In addition, a number of [Fe II] features are detected. In this phase the spectrum of SN 2009E more closely resembles those of SN 1987A and SN 1998A (Figure 8, top), although the spectral lines are significantly narrower than those of other 1987A-like events and are closer to those of sub-luminous, ⁵⁶Ni-poor SNe (Figure 8, bottom).

3. Constraining the progenitor of SN 2009E

3.1. The ejected oxygen mass

The strength of the [O I] λ 6300,6364 lines in the nebular spectra of core-collapse SNe can be used to roughly estimate the O mass ejected in the SN explosion (Uomoto 1986; Li & McCray 1992; Chugai 1994). This method has been applied for determining the O masses for a few type IIP SNe (see Maguire et al. 2010, and references therein). We first make an attempt to estimate the minimum O mass needed to produce the [O I] λ 6300–6364 feature with the relation between the O mass and the total flux of the doublet presented by Uomoto (1986). Using the nebular spectrum of SN 2009E, we measure an observed flux $F_{[OI]} \approx 3.35 \times 10^{-15}$ erg s⁻¹ cm⁻². Accounting for the reddening and distance estimates as mentioned in Section 2.1, we obtain for SN 2009E a minimum O mass in the range between 0.05 M $_{\odot}$ and 0.22 M $_{\odot}$ (assuming the extreme values of 3500 K and 4500 K, respectively as the temperature of the O-rich material, like in Maguire et al. 2010). As a comparison, Maguire et al. (2010) derived a minimum O mass range for SN 1987A of 0.3–1.1 M $_{\odot}$. The only other 1987A-like object with nebular spectra available is SN 1998A (Pastorello et al. 2005). Using the spectrum at phase \sim 344 days (see Figure 8, top), we obtain an O mass in the range 0.24–1.01 M $_{\odot}$.

In order to improve the O mass estimate, we adopt the method already used in Elmhamdi et al. (2003), which is based on the fact that the luminosity of the [O I] doublet in the nebular phase is known to be powered by the γ -rays produced in the radioactive decays of ⁵⁶Co to ⁵⁶Fe, and deposited in the O-rich ejecta. Since the mass of O in SN 1987A is reasonably

well-known (1.2–1.5 M $_{\odot}$, Li & McCray 1992; Chugai 1994; Kozma & Fransson 1998), we can derive the O masses of SNe 2009E and 1998A via comparison with the O mass of SN 1987A. We use the relation linking the O mass with the luminosities of the [O I] doublet⁷ and of the radioactively powered light curve tail, computed at similar phases (Elmhamdi et al. 2003):

$$L_{[OI]} = \eta_O \frac{M_O}{M_{exc}} L_{^{56}Co}, \quad (1)$$

where $L_{[OI]}$ and $L_{^{56}Co}$ are the luminosities of the [O I] doublet and of the radioactive tail (respectively), M_O is the mass of O, M_{exc} represents the whole excited mass in which the radioactive energy is deposited, and η_O is the efficiency of the transformation of the deposited energy into [O I] line radiation. Assuming that M_{exc} and η_O are similar in all 1987A-like events and noting that (since the late light curve of SN 2009E follows the ⁵⁶Co decay rate)

$$\frac{L_{^{56}Co}(1987A)}{L_{^{56}Co}(SN)} \propto \frac{M_{^{56}Ni}(1987A)}{M_{^{56}Ni}(SN)}, \quad (2)$$

from Equation 1, we obtain:

$$M_O(SN) = M_O(1987A) \times \frac{L_{[OI]}(SN) \times M_{^{56}Ni}(1987A)}{L_{[OI]}(1987A) \times M_{^{56}Ni}(SN)}. \quad (3)$$

Now we have all the ingredients needed to estimate the O mass in SNe 2009E and 1998A from Equation 3 using the information available for SN 1987A (Li & McCray 1992; Chugai 1994). For SN 2009E we obtain $M_O \approx 0.60$ – 0.75 M $_{\odot}$ (using as O mass for SN 1987A the extreme values of $M_{O,min} = 1.2$ M $_{\odot}$ and $M_{O,max} = 1.5$ M $_{\odot}$, respectively), while for SN 1998A we obtain $M_O \approx 1.18$ – 1.48 M $_{\odot}$. Therefore, with this method, we determine for the under-luminous SN 2009E an ejected mass of O that is a factor of 2 smaller than that of SN 1987A (note that for SN 2009E also the ⁵⁶Ni mass is a factor of \sim 2 smaller). In the case of SN 1998A we obtain an O mass that matches the values of SN 1987A, despite the former object ejected more ⁵⁶Ni.

According to the models presented by Woosley & Weaver (1995) and Thielemann et al. (1996), a star with main sequence mass of about 18–20 M $_{\odot}$ produces 1.2–1.5 M $_{\odot}$ of oxygen and a ⁵⁶Ni mass of 0.07–0.1 M $_{\odot}$. This is in excellent agreement with the values observed in SNe 1987A and 1998A. It is more difficult to provide an interpretation for the abundances displayed by SN 2009E (both M_O and $M_{^{56}Ni}$ are smaller by a factor 2 than those of SN 1987A), although we may tentatively guess that the lower O and ⁵⁶Ni masses would point toward a lower-mass main sequence star. We remark that the above estimates have been obtained under the simplifying assumption that M_{exc} and η_O were the same for SNe 1987A, 1998A and 2009E. This is not necessarily true, since we can reasonably expect a range of values for these parameters in 1987A-like events, and this would significantly affect our O mass estimates.

3.2. Modelling the data of SN 2009E

Other physical properties of SN 2009E (namely, the ejected mass, the progenitor initial radius and the explosion energy) have

⁷ We note that the luminosity of the [O I] doublet in SN 1987A and type IIP SNe remains almost constant over a long period during the nebular phase (between \sim 200–400 days, see e.g. Figure 8 in Elmhamdi et al. 2003).

been estimated by performing a model vs. data comparison using two codes that compute the bolometric light curve, the evolution of the ejecta velocity and the continuum temperature at the photosphere of a SN. The first code, based on a simplified semi-analytic treatment of the ejecta evolution (Zampieri et al. 2003), is used to perform a preparatory study in order to constrain the parameter space. The second code, that includes a more accurate treatment of radiative transfer and radiation hydrodynamics (Pumo et al. 2010; Pumo & Zampieri 2011), computes the tighter grid of models needed for the final comparison. This is similar to the procedure adopted for SN 2007od in Inserra et al. (2011).

The bolometric light curve was computed from the observed multicolor light curves using the assumptions on extinction and distance modulus reported in Section 2.1. We have adopted the explosion epoch estimated in Section 2.3 ($JD = 2454832.5_{-5}^{+2}$). Finally, we have assumed that SN 2009E had the same color evolution as SN 1987A (this is a reasonable assumption, see e.g. Figure 3), and hence

$$L(2009E) = L(1987A) \times \frac{L_{BVRI}(2009E)}{L_{BVRI}(1987A)}, \quad (4)$$

where L and L_{BVRI} are the bolometric and quasi-bolometric ($BVRI$) luminosities of the two SNe (bolometric data for SN 1987A were taken from Catchpole et al. 1987, 1988).

The best χ^2 fit to the bolometric light curve of SN 2009E obtained with the full radiation-hydrodynamics code returned values of a total (kinetic plus thermal) energy (E) of 0.6 foe, an initial radius (R_0) of 7×10^{12} cm, and an envelope mass (M_{ej}) of $19 M_\odot$ (see Figure 9). As a comparison, the fit with the semi-analytic code gave $E = 1.3$ foe, $R_0 = 6 \times 10^{12}$ cm, and $M_{ej} = 26 M_\odot$ (see again Figure 9). The parameters inferred from the two best-fits are in reasonable agreement. The envelope mass (and consequently the total energy) are slightly overestimated by the semi-analytic code as a consequence of the different mass distribution. Indeed, given the assumption of uniform density throughout the ejecta, the semi-analytic code tends to gather more mass (and hence more energy) in the external, faster-moving layers. The ^{56}Ni distribution also affects the mass estimate because, as a consequence of the simplified uniform distribution adopted in the semi-analytic code, less energy is released at the end of the photospheric phase and, hence, a more massive envelope is needed to sustain the recombination phase.

The ejected ^{56}Ni mass of $0.039 M_\odot$ that is adopted in the semi-analytic code is in an excellent agreement with that estimated in Section 2.3, whilst the one inferred from the radiation-hydrodynamic code is slightly higher ($0.043 M_\odot$). Since the latter code accounts also for the amount of material which (eventually) falls back onto the central remnant during the post-explosive evolution, the numerical simulations need a larger initial ^{56}Ni mass to reproduce the observed late-time light curve of SN 2009E.

In Figure 9 the evolutions of the photospheric velocity and temperature are also shown. The agreement between models and observations in the late photospheric phase is good, with possibly some discrepancy in matching the photospheric velocities at later times ($\gtrsim 4$ months). The decline of the model velocity profile is faster than that inferred from the observations, probably because some extra radioactive decay heating occurs in the inner part of the ejecta of SN 2009E as a consequence of a different (i.e. more centrally condensed) distribution of ^{56}Ni .

Finally, adopting a mass of the compact remnant of about $2 M_\odot$ (and assuming a negligible pre-SN mass loss), we derive

a final mass of $21 M_\odot$ for the progenitor of SN 2009E, which is slightly higher than our rough estimate obtained through the O mass estimate (Section 3.1).

4. SN 2009E and other 1987A-like events

Although 1987A-likeness was claimed for a number of objects in the past (e.g. SNe 1923A, 1948B and 1965L, Schmitz & Gaskell 1988; Young & Branch 1988; van den Bergh & McClure 1989), reasonable observational evidence exists for only a small number of events⁸. Additionally, for a few of them [SN 2004em, Gal Yam et al. (2007); SN 2005ci, Arcavi et al. (2009)] data are not published yet or are incomplete. Our limited 1987A-like sample includes the objects that are briefly described in Appendix A (and whose light curves are shown in Appendix B). The sample has been selected among objects that are spectroscopically classified as type II (without showing type II_n-like spectral features), and with light curves showing a slow rise to maximum.

Main parameters of the host galaxies of our sample of 1987A-like events are listed in Table 4. Remarkably, most SNe in our sample occurred in late-type galaxies (Scd or irregular). In addition, some of them were hosted by intrinsically faint (dwarf) galaxies, which are thought to have low-metallicities (see e.g. Young et al. 2010). However, at least half of the objects of our sample occurred in luminous spirals. Although luminous spirals are believed to be rather metal-rich, the 1987A-like events hosted in such galaxies occurred in peripheral -and hence more metal deficient- regions of the galaxies. Environments with low-to-moderate metallicity (slightly sub-solar) appear to be a fairly common characteristic for 1987A-like objects.

In Table 5 we report the values of some observational parameters for our SN sample. The magnitudes of the broad peaks seem to be correlated with the ejected ^{56}Ni masses (i.e. the objects with the brightest peak magnitudes are more ^{56}Ni -rich). The ^{56}Ni masses reported in Table 5 have been computed through a comparison between the late-time *uvoir* light curves of the different SNe with that of SN 1987A. The bolometric corrections were computed with reference to SN 1987A. The derived ^{56}Ni masses span a range between about $0.04 M_\odot$ and $0.13 M_\odot$ ⁹, similar to that observed in normal type IIP SNe, although cases of extremely ^{56}Ni -poor 1987A-like events (with ^{56}Ni masses of the order of $10^{-3} M_\odot$, Pastorello et al. 2004) have not been found so far.

Unfortunately, the sub-sample of 1987A-like SNe with an extensive data sets necessary for modelling is very small. This is necessary to constrain the properties of the progenitor stars. The rather large ejected mass, the moderate amount of synthesized ^{56}Ni , and the small initial radius found for SN 2009E (Section 3.2) fit reasonably well within the framework of a relatively compact and massive progenitor, and are in a good agreement with the results found in previous works on 1987A-like

⁸ Another type II SN, 2004ek, may show some similarity with this SN sub-group. Its light curve, published by Tsvetkov (2008), is rather peculiar, showing a sharp early-time peak, mostly visible in the bluer bands, followed by a pseudo-plateau lasting a couple of months. However, especially in the redder bands, a sort of delayed broad peak is visible, analogous to the one characterizing SNe 1982F and 2000cb. As major differences, SN 2004ek is significantly brighter ($M_V \approx -18$) and its spectrum, showing an $H\alpha$ mostly in emission (Filippenko et al. 2004) is rather peculiar. For this reason SN 2004ek has been rejected from our sample.

⁹ The lack of photometric points during the nebular phase did not allow us to obtain reliable estimates for the ^{56}Ni masses of SN 1982F.

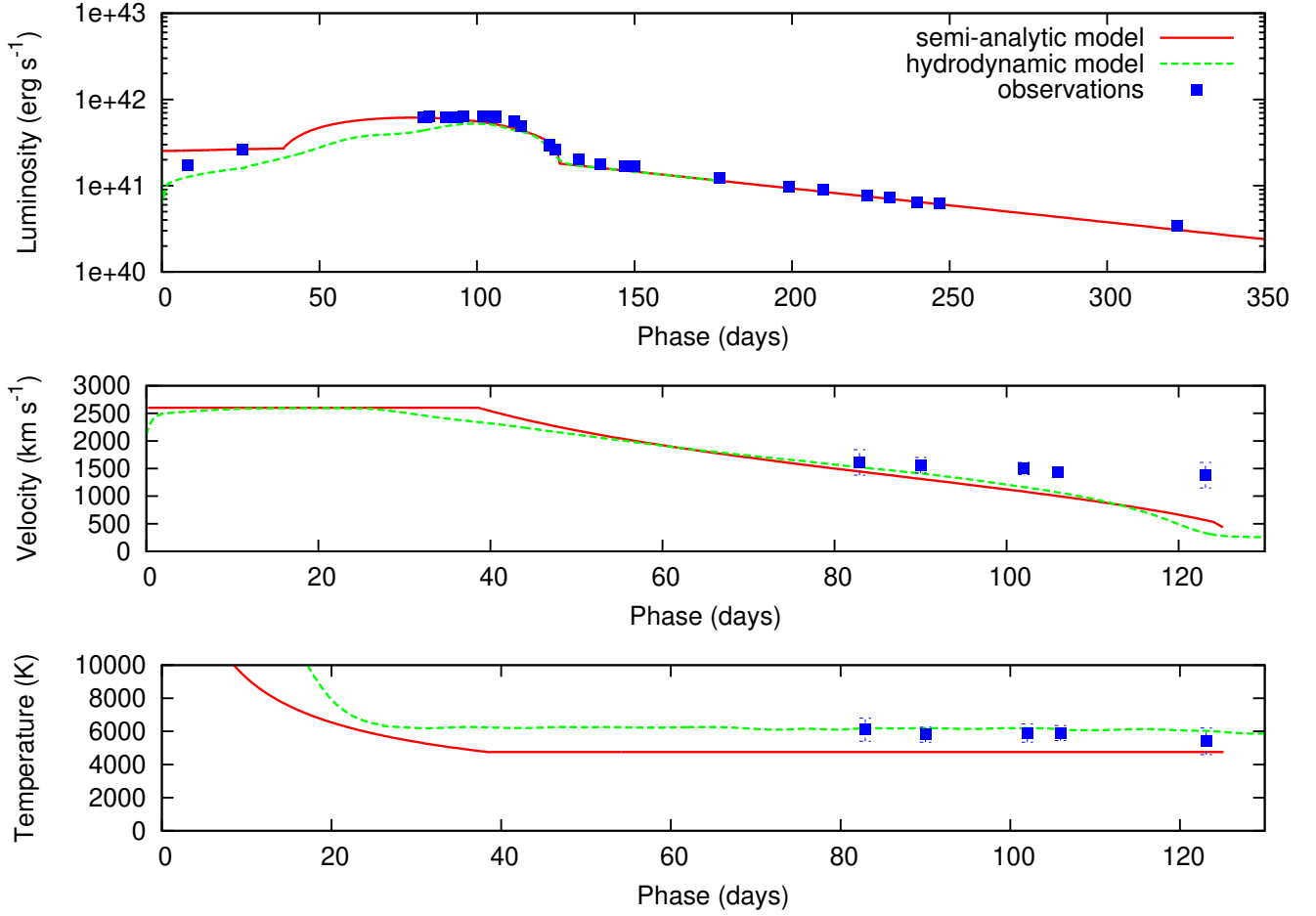


Fig. 9. Comparison of the evolution of the main observables of SN 2009E with the best-fit model computed with the relativistic radiation-hydrodynamics code (total energy 0.6 foe, initial radius 7×10^{12} cm, envelope mass $19 M_{\odot}$). The best-fit model computed with the semi-analytic code (total energy 1.3 foe, initial radius 6×10^{12} cm, envelope mass $26 M_{\odot}$) is also shown. Top, middle, and bottom panels show respectively the bolometric light curve, the photospheric velocity, and the photospheric temperature as a function of time. As a tracer for the photospheric velocity we measured the positions of the minimum of the P-Cygni profiles of the Sc II lines.

events (see Table 8 in Taddia et al. 2011). Using an older version of the semi-analytic modelling code than the one adopted here, Pastorello et al. (2005) obtained the following estimates for SNe 1987A and 1998A: $E(1987A) = 1.6$ foe, $E(1998A) = 5.6$ foe; $M_{ej}(1987A) = 18 M_{\odot}$, $M_{ej}(1998A) = 22 M_{\odot}$; $M_{^{56}Ni}(1987A) = 0.075 M_{\odot}$, $M_{^{56}Ni} = 0.11 M_{\odot}$; $R_0(1987A) \gtrsim 5 \times 10^{12}$ cm, $R_0(1998A) \gtrsim 6 \times 10^{12}$ cm. The major difference lies in the ejected ^{56}Ni masses of SNe 1987A and 1998A, which are $\times 2$ and $\times 3$ larger (respectively) than the one we have derived for SN 2009E (Section 3.2). Explosion parameters for a few additional 1987A-like SNe are also available in the literature (see also Taddia et al. 2011). Using a one-dimensional Lagrangian radiation-hydrodynamics code, Kleiser et al. (2011) derived the following parameters for the luminous 1987A-like SN 2000cb: $E(2000cb) = 2$ foe, $M_{ej}(2000cb) = 17.5 M_{\odot}$, $M_{^{56}Ni}(2000cb) = 0.10 M_{\odot}$ and $R_0(2000cb) = 3 \times 10^{12}$ cm. These values are slightly different from those derived by Utrobin & Chugai (2011) by modelling the spectroscopic and photometric data of SN 2000cb with a different hydrodynamic code. They inferred a presupernova radius of 2.4×10^{12} cm, an ejected mass of $22.3 M_{\odot}$, an

energy of 4.4 foe, and a mass of radioactive ^{56}Ni of $0.083 M_{\odot}$ ¹⁰. With a semi-analytic approach, Taddia et al. (2011) estimated relevant physical parameters for two 1987A-like events, SNe 2006V and 2006au: $E(2006V) = 2.4$ foe, $E(2006au) = 3.2$ foe; $M_{ej}(2006V) = 17.0 M_{\odot}$, $M_{ej}(2006au) = 19.3 M_{\odot}$; $M_{^{56}Ni}(2006V) = 0.127 M_{\odot}$, $M_{^{56}Ni}(2006au) \leq 0.073 M_{\odot}$; $R_0(2006V) = 5.2 \times 10^{12}$ cm, $R_0(2006au) = 6.3 \times 10^{12}$ cm.

It is evident that 1987A-like SN explosions have similar kinetic energies (a few $\times 10^{51}$ erg) and ejected masses (17 to $22 M_{\odot}$), whilst they appear to span a factor of 3 in ^{56}Ni masses (see also Table 8 in Taddia et al. 2011, for a summary of the parameters of the best-studied 1987A-like events). It is intriguing to note that the modelling reported above suggest that *all the 1987A-like SNe would be produced by the explosions of BSG progenitors that have initial radii ranging between 35 and 90 R_{\odot} , and with final masses around $20 M_{\odot}$* . These progenitor masses are systematically higher than those estimated for the RSG progenitors of classical SNe IIP (e.g. Smartt et al. 2009).

¹⁰ Note, however, that the distance moduli adopted by Pastorello et al. (2005) for the host of SN 2009E ($\mu = 32.41$) and by Kleiser et al. (2011) and Utrobin & Chugai (2011) for the host of SN 2000cb ($\mu = 32.39$) are different from those adopted here and reported in Table 4.

Table 4. Parameters of the explosion sites of the 1987A-like SNe. In column 3 we report the morphologic types of the host galaxies, in columns 4 and 5 the adopted distance moduli and Galactic extinctions from Schlegel et al. (1998), in column 6 the *B*-band absolute magnitudes of the galaxies, in column 7 the ratios between the deprojected position of the SN and r_{25} computed following Hakobyan et al. (2009), in column 8 the oxygen abundances from Pilyugin’s relation (computed at $0.4r_{25}$, Pilyugin et al. 2004), in column 9 the corrected oxygen abundances from Pilyugin’s relation computed at the deprojected SN distance.

SN	Host galaxy	Type ¹	μ^2	$A_{B,MW}$	M_B	d_{SN}^3/r_{25}	P04	P04 corr.
1909A	NGC 5457	SABc	29.34 ³	0.037	-21.01	1.11 ⁹	8.59	8.30 ¹⁰
1982F	NGC 4490	SBcd	29.92	0.093	-20.25	0.23	8.53	8.60 ¹¹
1987A	LMC	SBm	18.50 ⁴	0.324	-18.02	-	8.31	-
1998A	IC 2627	SABc	32.19	0.518	-20.03	0.66	8.51	8.41
1998bt	A132541-2646	-	36.41 ⁵	0.244	-13.25	-	7.98	-
2000cb	IC 1158	SABc	32.68 ⁶	0.491	-19.34	0.93	8.46	8.24
NOOS-005	2MASX J05553978-6855381	S	35.46	0.656 ⁸	-20.01	1.26	8.51	8.17
2004em	IC 1303	Sc	34.07	0.466	-19.73	0.96	8.49	8.26
2005ci	NGC 5682	Sb	32.73	0.141	-18.07	0.66	8.36	8.26
2006V	UGC 6510	SABc	34.36 ⁷	0.125	-20.97	1.31	8.59	8.22
2006au	UGC 11057	Sc	33.38 ⁷	0.742	-20.64	0.90	8.56	8.36
2009E	NGC 4141	SBc	32.38	0.086	-17.75	0.68	8.33	8.22

¹ Morphologic type as quoted by HyperLeda.

² Unless otherwise specified, distance moduli are computed from HyperLeda’s v_{vir} , adopting $H_0 = 72 \text{ km s}^{-1} \text{ Mpc}^{-1}$.

³ Distance computed from the tip of the red giant branch (TRGB, Rizzi et al. 2007). Cepheid distances are found to be too sensitive to metallicity. The metallicity correction is even more crucial in the case of NGC 5457 where inner metal-poor and outer metal-rich cepheids give uncorrected distance moduli that may differ by 0.3-0.4 mags (Saha et al. 2006).

⁴ For LMC we adopted a cepheid distance, well consistent with that derived from the TRGB (Sakai et al. 2004; Rizzi et al. 2007).

⁵ SN 1998bt was discovered in the course of the Mount Stromlo Abell cluster supernova search (Germany et al. 2004). Unfortunately, no spectroscopic classification exists for this SN.

According to Germany et al. (2004), there is a very faint host galaxy at the position of SN 1998bt, but no spectrum was ever obtained of this galaxy. We assume that the galaxy hosting SN 1998bt belongs to a cluster monitored by the search whose average redshift is $z = 0.046$.

⁶ Average EPM distance from Table 4.1 of Hamuy (2001).

⁷ Distance as in Taddia et al. (2011), but obtained adopting an Hubble Constant $H_0 = 72 \text{ km s}^{-1} \text{ Mpc}^{-1}$.

⁸ This galaxy is behind LMC, so the extinction reported here includes both Galaxy and LMC contributions (see text for references).

⁹ Computed using the position angle provided by Jarrett et al. (2003).

¹⁰ Other sources give $12+\log(\text{O}/\text{H}) \approx 7.7\text{--}7.8$ at the position of SN 1909A (Kennicutt et al. 2003; Pilyugin et al. 2004; Bresolin 2007).

¹¹ An alternative estimate from Pilyugin & Thuan (2007) gives $12+\log(\text{O}/\text{H}) = 8.35$.

5. Rate of 1987A-like events

While it would be of interest to know the relative rate of 1987A-like events vs. normal type II SNe, the heterogeneous properties of this class and the uncertainties in the sample population from which the events reported in Table 4 are extracted prevent us from providing any accurate estimates. With the aim to derive an educated guess, the completeness of the SN searches with respect to the 1987A-like objects list can be assessed by comparing the distance modulus distribution of 1987A-like events with that of a suitable reference sample. For the latter, we extracted from the Asiago Supernova Catalogue the list of all type II SNe. If we limit the distance modulus to about 35 mag (at higher redshift incompleteness appears to be significant) it seems that 1987A-like events would account for less than 1.5% of all type II SNe. This value, that can be considered as a lower limit for the relative rate of 1987A-like events, is very similar to that derived by Kleiser et al. (2011) based on the two 1987A-like SNe discovered by the LOSS.

However, the identification of 1987A-like events demands a fairly good light curve coverage that is not available for many of the type II SNe listed in the catalogue. Actually, reasonably good light curves of type II (IIP, IIL, I Ib, II n) SNe exist for about 300 objects. This approximate estimate was obtained including both SNe whose data have been published in literature, and SNe spectroscopically classified whose photometric follow-up information is available in public pages of current SN monitoring

programs¹¹. From this estimate, we infer that 1987A-like events comprise about 4% of all type II SNe. This has to be considered as a sort of upper limit, since we expect that the astronomical community has been investing more efforts to follow peculiar 1987A-like SNe rather than other type II SN sub-types because of their intrinsic rarity. Therefore, we estimate that SNe photometrically similar to SN 1987A comprise between ~ 1.4 and 4% of all type II SNe, corresponding to about 1-3% of all core-collapse SNe in a volume-limited sample (e.g. Smartt et al. 2009; Li et al. 2011).

6. Summary

New data for the peculiar type II SN 2009E have been presented. Its light curve is very similar to that of SN 1987A, with a few main differences: the light curve peak is shifted in phase by about +10 days with respect to that of SN 1987A, its luminosity is fainter than that of SN 1987A and the amount of ^{56}Ni deduced from the luminosity of the radioactive tail is about $0.04M_{\odot}$. This is the lowest ejected ^{56}Ni mass estimated for any 1987A-like event studied so far. The spectra of SN 2009E appear to be different from those of SN 1987A (and similar events), while they

¹¹ For example, the ESO/TNG large program on Supernova Variety and Nucleosynthesis Yields (<http://graspa.oapd.inaf.it/>), the Caltech Core-Collapse Program (<http://www.astro.caltech.edu/~avishay/cccp.html>) or the Carnegie Supernova Project (<http://csp1.lco.cl/~cspuser1/PUB/CSP.html>)

Table 5. Adopted parameters for 1987A-like SNe. The total extinction is reported in column 2, the JD of explosion in column 3, the bands in column 4, the JD of the maximum light in column 5, the phase of the broad maximum (in days past explosion) in column 6, the apparent and absolute peak magnitudes in columns 7 and 8 (respectively) and the ^{56}Ni mass in column 9. The extinction law of Cardelli et al. (1989) was used in these estimates. The explosion epochs have been determined through a comparison with the light curves of SN 1987A.

SN	$E_{\text{tot}}(\text{B-V})^a$	$JD_{\text{expl.}}$	Band	JD_{peak}	$t-t_0$ (days)	$m_{\text{peak}}(\text{filter})$	M_{peak}	$M(^{56}\text{Ni})$	Sources
1909A	0.009	2418310 \pm 30	<i>B</i>	2418383 \pm 7	73 \pm 31	14.47 \pm 0.30	-15.91	0.13 M_{\odot} ^b	1
1982F	0.022	2445014 \pm 15	<i>B</i>	2445087 \pm 4	73 \pm 16	16.40 \pm 0.02	-13.61	–	2,3,4
			<i>V</i>	2445097 \pm 3	83 \pm 15	14.95 \pm 0.10	-15.04		
1987A	0.19	2446849.816 ^c	<i>B</i>	2446932.0 \pm 1.1	82.2 \pm 1.1	4.52 \pm 0.01	-14.77	0.075 M_{\odot}	5
			<i>V</i>	2446932.2 \pm 1.0	82.4 \pm 1.0	2.96 \pm 0.01	-16.13		
			<i>R</i>	2446933.6 \pm 1.0	83.8 \pm 1.0	2.27 \pm 0.01	-16.67		
			<i>I</i>	2446935.2 \pm 0.9	85.4 \pm 0.9	1.90 \pm 0.01	-16.88		
1998A	0.120	2450801 \pm 4	<i>B</i>	2450876.3 \pm 7.4	75.3 \pm 8.4	17.59 \pm 0.13	-15.12	0.09 M_{\odot}	6
			<i>V</i>	2450885.4 \pm 8.3	84.4 \pm 9.2	16.31 \pm 0.09	-16.28		
			<i>R</i>	2450885.6 \pm 3.9	84.6 \pm 5.6	15.73 \pm 0.06	-16.78		
			<i>I</i>	2450889.2 \pm 5.5	88.2 \pm 6.8	15.37 \pm 0.07	-17.05		
1998bt	0.057	2450831 \pm 30	<i>V</i>	2450905 \pm 6	74 \pm 31	19.81 \pm 0.05	-16.79		7,0
			<i>R</i>	2450908 \pm 8	77 \pm 31	19.38 \pm 0.08	-17.18		8,0
2000cb	0.112	2451653.8 \pm 1.4	<i>B</i> ^d			18.23 \pm 0.02	-14.94	0.11 M_{\odot}	8,9,10
			<i>V</i>	2451714.6 \pm 4.7	60.8 \pm 4.9	16.58 \pm 0.02	-16.47		
			<i>R</i>	2451725.2 \pm 2.1	71.4 \pm 2.5	15.95 \pm 0.02	-17.03		
			<i>I</i>	2451729.0 \pm 1.4	75.2 \pm 2.0	15.56 \pm 0.02	-17.34		
NOOS-005	0.160	2452855 \pm 15	<i>I</i>	2452939.5 \pm 2.7	84.5 \pm 15.2	18.22 \pm 0.02	-17.51	0.13 M_{\odot}	0
2005ci	0.033?	2453521 \pm 3	<i>unf.</i>			<17.5	<-15.3		10
2006V ^e	0.029	2453748 \pm 4	<i>B</i>	2453823.7	75.7	18.29 \pm 0.01	-16.20	0.13 M_{\odot}	11
2006au ^e	0.312	2453794 \pm 9	<i>B</i>	2453865.5	71.5	18.63 \pm 0.02	-16.06	<0.07 M_{\odot}	11
2009E	0.04	2454832.5 \pm 2.0	<i>B</i>	2454919.0 \pm 6.5	86.5 \pm 6.8	18.01 \pm 0.03	-14.54	0.04 M_{\odot}	0
			<i>V</i>	2454924.9 \pm 5.9	92.4 \pm 6.2	16.76 \pm 0.04	-15.74		
			<i>R</i>	2454928.3 \pm 2.8	95.8 \pm 3.4	16.25 \pm 0.02	-16.21		
			<i>I</i>	2454928.3 \pm 6.0	95.8 \pm 6.3	15.98 \pm 0.03	-16.46		

^a The SN extinction is computed accounting for both Milky Way (Schlegel et al. 1998, see also Column 3 of Table 4) and host galaxy reddening components; in the case of NOOS-005, since the host galaxy is projected behind LMC, we also accounted for the contribution of LMC.

^b Computed using the B-band detections at days +429 and +432, and assuming the same colour evolution as SN 1987A. Using the detection at day +216, we would obtain $M(^{56}\text{Ni}) \approx 0.35M_{\odot}$.

^c Alexeyev & Alexeyeva (2008) and references therein.

^d The broad delayed maximum typical of 1987A-like SNe is not visible in the B band; here we report the magnitude of the pseudo-plateau visible after the early time B-band maximum.

^e For a comprehensive information on the multi-band light curve parameters, see Table 7 of Taddia et al. (2011).

0 = This paper; 1 = Sandage & Tammann 1974; 2 = Yamagata & Iye 1982; 3 = Tsvetkov 1984; 4 = Tsvetkov 1988; 5 = Whitelock et al. 1989 (and references therein); 6 = Pastorello et al. 2005; 7 = Germany et al. 2004; 8 = Hamuy 2001; 9 = Hamuy & Pinto 2002; 10 = Kleiser et al. 2011; 11 = Taddia et al. 2011.

share major similarities with those of sub-luminous, ^{56}Ni -poor SNe IIP (e.g. SN 2005cs) in terms of line velocities and relative line strengths.

In analogy with what has been deduced for SN 1987A, also the observed properties of SN 2009E are consistent with those expected from the explosion of a BSG star. Modelling the data of SN 2009E, we obtained a relatively under-energetic explosion ($E = 0.6$ foe), an initial radius of of 7×10^{12} cm and an ejected mass of $19M_{\odot}$, pointing toward a relatively high-mass precursor star ($21M_{\odot}$), very similar to the BSG progenitor inferred for SN 1987A.

Finally, we compared the observed properties of a dozen of 1987A-like SNe available in the literature, and found that this subgroup of type II SNe shows significant variety in the explosion parameters and in the characteristics of the host galaxies (although they seem to prefer moderately metal-poor environments). This would suggest for these objects a distribution in the space of parameters which is similar to that observed in more classical type IIP SNe, although they are intrinsically rare ($\lesssim 3\%$ of all core-collapse SNe in a volume-limited sample).

Acknowledgements. This work is based in part on observations collected at the Italian 3.58-m Telescopio Nazionale Galileo (TNG), the 2.56-m Nordic Optical Telescope, the 2.2-m Telescope of the Centro Astronómico Hispano Alemán (Calar Alto, Spain) and the 1.82-m Copernico Telescope on Cima Ekar (Asiago, Italy). The TNG is operated by the Fundación Galileo Galilei of the Instituto Nazionale di Astrofisica at the Spanish Observatorio del Roque de los Muchachos of the Instituto de Astrofísica de Canarias. We thank the support astronomers at the TNG, the 2.2-m Telescope at Calar Alto and the Nordic Optical Telescope for performing the follow-up observations of SN 2009E. SB, FB, EC, MT and AH are partially supported by the PRIN-INAF 2009 with the project ‘Supernovae Variety and Nucleosynthesis Yields’. MLP acknowledges financial support from the Bonino-Pulejo Foundation. SM acknowledges financial support from the Academy of Finland (project: 8120503). We are grateful to the TriGrid VL project and the INAF-Astronomical Observatory of Padua for the use of computer facilities.

EP acknowledges the project SkyLive of the Unione Astrofili Italiani (UAI) and the SkyLive Remote Facility - Osservatorio B40 SkyLive, Catania, Italy (<http://www.skylive.it>). We thank the amateur astronomers of the Associazione Astronomica Isaac Newton (<http://www.isaacnewton.it>) and of the Associazione Astronomica Cortina (<http://www.cortinastelle.it/>) for providing images of SN 2009E obtained during the SMMSS and CROSS supernova search programs: G. Iacopini (Osservatorio di Tavoia, S. Maria a Monte, Pistoia), R. Mancini and F. Briganti (Stazione di Osservazione di Gavena, Cerreto Guidi, Italy), A. Dimai (Osservatorio di Col Druscé, Cortina, Italy). We also thank J.M. Llapasset, O. Trondal, Boyd, for sharing their images with us, I. Bano and A. Englaro

(Osservatorio Astronomico Polse di Cugnes) for their help with observations, A. Siviero for allowing ToO observations of SN 2009E at the 1.82-m Telescope of Asiago (Mt. Ekar, Italy) and T. Iijima for providing us the B&C spectrum obtained at the 1.22-m Galileo Telescope (Osservatorio Astrofisico di Asiago). AP is grateful to Mario Hamuy, Io Kleiser, Dovi Poznanski and Lisa Germany for sharing their data of SNe 2000cb and 1998bt.

This manuscript made wide use of information contained in the Bright Supernova web pages (maintained by D. Bishop), as part of the Rochester Academy of Sciences (<http://www.RochesterAstronomy.org/snimages/>). We also used information collected from the the web site SNAude des Supernovae (<http://www.astrosurf.com/snaude/>). The paper is also based in part on data collected at the Akeno 50 cm Telescope (Akeno Observatory/ICRR, Yamanashi, Japan) and obtained from the SMOKA, which is operated by the Astronomy Data Center, National Astronomical Observatory of Japan; and at the Faulkes North Telescope and obtained through the Faulkes Telescopes Data Archive.

References

- Aikman, C., & Newton, J. 1982, IAU Circ. 3690, 2
- Aldering, G., & Conley, A. 2000, IAU Circ. 7410, 3
- Alexeyev, E. N., & Alexeyeva, L. N. 2008, *AstL*, 34, 745
- Arcavi, I., Gal-Yam, A., Kiewe, M., et al. 2009, American Astronomical Society meeting 214, 604.01
- Armstrong, M. 2004, CBET, 82, 1
- Arnett, W. D., Bahcall, J. N., Kirshner, R. P., & Woosley, S. E. 1989, *ARA&A*, 27, 629
- Baba, H., Yasuda, N., Ichikawa, S., et al. 2002, *Development of the Subaru-Mitaka-Okayama-Kiso Archive System*, ADASS XI, eds. D. A. Bohlender, D. Durand, & T. H. Handley, ASP Conference Series, Vol.281, 298
- Benetti, S., Turatto, M., Balberg, S., et al. 2001, MNRAS, 322, 361
- Blanc, N., Copin, Y., Gangler, E., et al. 2006, *Astron. Tel.* 762, 1
- Blondin, S., Modjaz, M., Kirshner, R., Challis, P., & Calkins, M. 2006, CBET 392, 1
- Blondin, S., Barbon, R., Pastorello, A., & Calkins, M. 2008, CBET 1300, 1
- Bionta, R. M., Blewitt, G., Bratton, C. B., Caspere, D., & Ciocio, A. 1987, *Phys. Rev. Lett.*, 58, 1494
- Boles, T. 2008, CBET 1239, 1
- Boles, T. 2009, CBET 1648
- Borkowski, K. J., Blondin, J. M., & McCray, R. 1997, *ApJ*, 477, 281
- Bresolin, F. 2007, *ApJ*, 656, 186
- Cardelli, J. A., Clayton, G. C., & Mathis, J. S. 1989, *ApJ*, 345, 245
- Catchpole, R. M., Menzies, J. W., Monk, A. S., et al. 1987, MNRAS, 229, P15
- Catchpole, R. M., Whitelock, P. A., Feast, M. W., et al. 1988, MNRAS, 231, P75
- Catchpole, R. M., Whitelock, P. A., Menzies, J. W., et al. 1989, MNRAS, 237, P55
- Chen, Y.-T., Yang, M., & Lin, C.-S. 2006, CBET 390, 1
- Chugai, N. N. 1994, *ApJ*, 428, L17
- Elmhamdi, A., Danziger, I. J., Chugai, N. N., et al. 2003, MNRAS, 338, 939
- Filippenko, A. V., Ganeshalingam, M., & Swift, B. J. 2004, IAU Circ. 8411, 1
- Gal Yam, A., Cenke, S. B., Fox, D. B., Leonard, D. C., Moon, D.-S., Sand, D. J., & Soderberg, A. M. 2007, AIPC, 924, 297
- Gilmozzi, R., Cassatella, A., Clavel, J., et al. 1987, *Nature*, 328, 318
- Germany, L., 1998, IAU Circ. 6898
- Germany, L. M., Reiss, D. J., Schmidt, B. P., Stubbs, C. W., & Suntzeff, N. B. 2004, *A&A*, 415, 863
- Hakobyan, A. A., Mamom, G. A., Petrosian, A. R., Kunth, D., & Turatto, M. 2009, *A&A*, 508, 1259
- Hamuy, M., Suntzeff, N. B., Gonzales, R., & Martin, G. 1988, *AJ*, 95, 63
- Hamuy, M., & Suntzeff, N. B. 1990, *AJ*, 99, 1146
- Hamuy, M. 2001, Ph.D. Thesis, Univ. of Arizona
- Hirata, K., Kajita, T., Koshihara, M., Nakahata, M., & Oyama, Y. 1987, *Phys. Rev. Lett.*, 58, 1490
- Insera, C., Turatto, M., Pastorello, A., et al. 2011, MNRAS, in press (arXiv:1102.5468)
- Jarrett, T. H., Chester, T., Cutri, R., Schneider, S. E., & Huchra, J. P. 2003, *AJ*, 125, 525
- Jha, S., Challis, P., & Kirshner, R. 2000, IAU Circ. 7410, 2
- Jones, D. H., Read, M. A., Saunders, W. 2009, MNRAS, 399, 683
- Kennicutt, R. C. Jr., Bresolin, F., & Garnett, D. R. 2003, *ApJ*, 591, 801
- Kewley, L. J., Jansen, R. A., & Geller, M. J. 2005, *PASP*, 117, 227
- Kleiser, I. K. W., Poznanski, D., Kasen, D., et al. 2011, MNRAS, 415, 372
- Kozma, C., & Fransson, C. 1998, *ApJ*, 497, 431
- Landolt, A. U. 1992, *AJ*, 104, 340
- Li, H., & McCray, R. 1992, *ApJ*, 387, 309
- Li, W., Leaman, J., Chornock, R., et al. 2011, MNRAS, 412, 1441
- Madison, D., Li, W. 2005, IAU Circ. 8541, 1
- Madison, D., Li, W., & Filippenko, A. 2008, CBET 1239, 2
- Maguire, K., di Carlo, E., Smartt, S. J., et al. 2010, MNRAS, 404, 981
- Mazzali, P. A., Lucy, L. B., & Butler, K. 1992, *A&A*, 258, 399
- Mazzali, P. A., & Chugai, N. N. 1995, *A&A*, 303, 118
- Menzies, J. W., Catchpole, R. M., van Vuuren, G., et al., 1987, MNRAS, 227, 39
- Modjaz, M., Kirshner, R., & Challis, P. 2005, IAU Circ. 8542, 2
- Navasardyan, H., Benetti, S., Bufano, F., & Pastorello, A. 2009, CBET 1738, 1
- Papenkova, M., & Li, W. 2000, IAU Circ. 7410, 1
- Pastorello, A., Zampieri, L., Turatto, M., et al. 2004, MNRAS, 347, 74
- Pastorello, A., Baron, E., Branch, D., et al. 2005, MNRAS, 360, 950
- Pastorello, A., Sauer, D., Taubenberger, S., et al. 2006, MNRAS, 370, 1752
- Pastorello, A., et al. 2008, MNRAS, 389, 131
- Pastorello, A., Valenti, S., Zampieri, L., et al. 2009, MNRAS, 394, 2266
- Patat, F., Barbon, R., Cappellaro, E., & Turatto, M. 1994, *A&A*, 282, 731
- Phillips, M. M., Heathcote, S. R., Hamuy, M., & Navarrete, M. 1988, *AJ*, 95, 1087
- Phillips, M. M., Hamuy, M., Heathcote, S. R., Suntzeff, N. B., & Kirhakos, S. 1990, *AJ*, 99, 1133
- Pilyugin, L. S., Vílchez, J. M., & Contini, T. 2004, *A&A*, 425, 849
- Pilyugin, L. S., & Thuan, T. X. 2007, *ApJ*, 669, 299
- Poznanski, D., Ganeshalingam, M., Silverman, J. M., & Filippenko, A. V. 2011, MNRAS, 415, L81
- Pumo, M. L., Zampieri L., & Turatto M., 2010, *Mem. S.A.It. Suppl.*, 14, 123
- Pumo, M. L., & Zampieri L. 2011, *ApJ*, accepted (arXiv:1108.0688)
- Prosperi, E., & Hurst, G. H. 2009, CBET 1734
- Pun, C. S. J., Kirshner, R. P., Sonneborn, G., et al. 1995, *ApJS*, 99, 223
- Rizzi, L., Tully, R. B., Makarov, D., Makarova, L., Dolphin, A. E., Sakai, S., & Shaya, E. J. 2007, 661, 815
- Saha, A., Thim, F., Tammann, G. A., Reindl, B., & Sandage, A. 2006, *ApJS*, 165, 108
- Sakai, S., Ferrarese, L., Kennicutt, R. C., & Saha, A. 2004, *ApJ*, 608, 42
- Sandage, A., & Tammann, G. A., 1974, *ApJ*, 194, 223
- Schlegel, D. J., Finkbeiner, D. P., & Davis, M. 1998, *ApJ*, 500, 525
- Schmitz, M. F., & Gaskell, C. M. 1988, in *Supernova 1987A in the Large Magellanic Cloud*, ed. M. Kafatos and A. Michalitsianos (Cambridge: Cambridge University Press), p. 112
- Smartt S. J., Eldridge J. J., Crockett R. M., & Maund J. R. 2009, MNRAS, 395, 1409
- Sonneborn, G., Altner, B., & Kirshner, R. P. 1987, *ApJ*, 323, L35
- Taddia, F., et al. 2011, *A&A*, accepted (arXiv:submit/0355695)
- Thielemann, F.-K., Nomoto, K., & Hashimoto, M.-A. 1996, *ApJ*, 460, 408
- Tsujimoto, T., & Shigeyama, T. 2001, *ApJ*, 561, L97
- Trondal, O., Luckas, P., & Schwartz, M. 2006, CBET 426, 1
- Tsvetkov, D. Y. 1984, *Astr. Tsirk.*, 1346, 1
- Tsvetkov, D. Y. 1988, *PZ*, 22, 653
- Tsvetkov, D. Yu., Volnova, A. A., Shulga, A. P., Korotkiy, S. A., Elmhamdi, A., Danziger, I. J., & Ereshko, M. V. 2006, *A&A*, 460, 769
- Tsvetkov, D. Y. 2008, *PZ*, 28, 3
- Turatto, M., Mazzali, P. A., Young, T. R., et al. 1998, *ApJ*, 498, 129
- Turatto, M., Cappellaro, E., & Benetti, S. 2003, in Leibundgut B., Hillebrandt W., eds, *Proc. to the ESO/MPA/MPPE Workshop (an ESO Astrophysics Symp.)*, *From Twilight to Highlight: the Physics of Supernovae*, Springer-Verlag, Berlin, p. 200
- Udalski, A. 2003, *Acta Astron.*, 53, 291
- Udalski, A., Szymański, M. K., Soszyński, I., & Poleski, R. 2008, *Acta Astron.*, 58, 69
- Uomoto, A. 1986, *ApJ*, 310, L35
- Utrobin, V. P., & Chugai, N. N. 2005, *A&A*, 441, 271
- Utrobin, V. P., & Chugai, N. N. 2011, *A&A*, accepted (arXiv:1107.2145)
- van den Bergh, S., & McClure, R. D. 1989, *ApJ*, 347, L29
- Whitelock, P. A., Catchpole, R. M., Menzies, J. W., et al., 1988, MNRAS, 234, 5
- Whitelock, P. A., Catchpole, R. M., Menzies, J. W., et al., 1989, MNRAS, 240, 7
- Williams, R. E. 1987, *ApJ*, 320, L117
- Williams, A., Woodings, S., Martin, R., Verveer, A., & Biggs, J. 1998, IAU Circ. 6805, 2
- Woodings, S. J., Williams, A. J., Martin, R., Burman, R. R., & Blair, D. G. 1998, MNRAS, 301, L5
- Woosley, S. E. 1988, *ApJ*, 330, 218
- Woosley, S. E., & Weaver, T. A. 1995, *ApJS*, 101, 181
- Yamagata, T., & Iye, M. 1982, *IBVS*, 2204, 1
- Young, T. R., & Branch, D. 1988, *Nature*, 333, 305
- Young, D. R., Smartt, S. J., Valenti, S., et al. 2010, *A&A*, 512, 70
- Zampieri, L., Pastorello, A., Turatto, M., et al. 2003, MNRAS, 338, 711
- Zaritsky, D., Harris, J., Thompson, I. B., & Grebel, E. K. 2004, *AJ*, 128, 1606

Appendix A: Basic information on the sample of SN 1987-like transients

1. **SN 1987A** is the prototype of this family of H-rich core-collapse SNe, and -since it exploded in the nearby Large Magellanic Cloud- it is the best studied SN ever. The SN was discovered on 1987 February 24th by Shelton. Strong constraints on the time of the core-collapse came from the detection of a neutrino burst on February 23.316 UT by IMB and Kamiokande II (Bionta et al. 1987; Hirata et al. 1987). Extensive data sets at all wavelengths are provided by a large number of publications (e.g. Menzies et al. 1987; Catchpole et al. 1987, 1988, 1989; Whitelock et al. 1988, 1989; Hamuy et al. 1988; Phillips et al. 1988, 1990; Pun et al. 1995). More recent papers have unveiled the complex structure of the circumstellar environment of SN 1987A and its interaction with the SN ejecta (e.g. Borkowski et al. 1997). SN 1987A is one of the few objects for which we have robust constraints on the nature of the progenitor star. Pre-explosion images of the source at the SN position (Sk -69 202) showed it to be a blue (B3 I) supergiant (Gilmozzi et al. 1987; Sonneborn et al. 1987) whose mass is estimated to be around $20 M_{\odot}$ (see Arnett et al. 1989, for a review). A small initial radius of the progenitor star is also used to explain the unusual, slow rise to maximum of the light curves of SN 1987A. In this paper we adopt as distance modulus of LMC and as total reddening toward SN 1987A the values of $\mu = 18.50$ mag (Sakai et al. 2004) and $E(B - V) = 0.19$ mag (Arnett et al. 1989).
2. **SN 1909A** is a historical SN that exploded in M101. Its photometric evolution shows striking similarity with that of SN 1987A (Young & Branch 1988; Patat et al. 1994, see also Appendix B). A well-sampled light curve from photographic plates rescaled to the B-band system was published by Sandage & Tammann (1974). We assume negligible extinction toward SN 1909A and a distance modulus of $\mu = 29.34$ mag (Rizzi et al. 2007, see Table 4 for details). Although multiband observations are missing for this event, the B-band absolute magnitude at maximum ($M_B \approx -15.9$, see Table 5) suggests that SN 1909A is one of the intrinsically brightest SNe in our sample.
3. **SN 1982F** in NGC 4490 is a poorly followed under-luminous type II SN. Sparse data around maximum from photographic plates were published by Yamagata & Iye (1982) and Tsvetkov (1984, 1988). The light curves share remarkable similarity with SN 2000cb (see below), more than with SN 1987A. No spectrum exists for this object to our knowledge.
4. **SN 1998A** is a well studied 1987A-like event which exploded in a spiral arm of the SBc galaxy IC 2627. The SN was discovered on 1998 January 6 by the Automated Supernova Search Program of the Perth Astronomy Research Group (PARG, Williams et al. 1998). Optical photometry and spectroscopy were published by Woodings et al. (1998) and Pastorello et al. (2005). Adopting the HyperLeda recessional velocity corrected for local infall onto Virgo $v_{Vir} = 1976 \text{ km s}^{-1}$, we obtain a distance of 27.4 Mpc ($\mu = 32.19$ mag). Since there was no evidence of additional extinction in the host galaxy, we adopt the same total reddening estimate as in Pastorello et al. (2005), i.e. $E(B - V) = 0.12$ mag.
5. **SN 1998bt** was discovered in the Abell cluster 1736 by the Mount Stromlo Abell cluster supernova search team on March 10, 1998 (Germany 1998). Initially, no background galaxy was seen to be associated with the SN. However, subsequent deep imaging of the SN field revealed a very faint parent galaxy of $R = 23.4$ (Germany et al. 2004). Unfortunately, spectroscopic classification for this SN does not exist. However, the overall behaviour of the light curve (see Figure B.1) is reminiscent of that of SN 1987A.
6. **SN 2000cb** in IC 1158 is one of the best followed 1987A-like events in our sample. Discovered on April 27.4 2000 using the 0.8-m Katzman Automatic Imaging Telescope (KAIT, Papenkova & Li 2000), it was classified as a young type II SN by Jha et al. (2000) and Aldering & Conley (2000). Optical photometric and spectroscopic observations have been presented by Hamuy (2001) and Kleiser et al. (2011). The photometric evolution of SN 2000cb is different from that of SN 1987A. The light curve in the B band shows a maximum at ≈ 40 days past core-collapse, followed by a slow decline up to 60 days and a short pseudo-plateau. At about 90 days a steep post plateau decline to the radioactive tail is visible, as in normal type IIP SNe. The evolution in the VRI bands is somewhat different, showing broad light curve peaks at 60–80 days (depending on the band) after core-collapse (Hamuy 2001; Kleiser et al. 2011). The light curve peaks are significantly broader than those of SN 1987A. We adopted the observed parameters of SN 2000cb as presented in Hamuy (2001). The explosion epoch, the adopted distance and the total reddening are those of Hamuy (2001). Their values are listed in Tables 4 and 5.
7. **OGLE-2003-NOOS-005** never had a SN designation. It was discovered by the Optical Gravitational Lensing Experiment (OGLE, Udalski 2003) collaboration at $\alpha = 5^h55^m38^s.07$ and $\delta = -68^\circ55'47''.1$ (J2000.0). It exploded in a faint spiral galaxy labelled by the NED database as 2MASX J05553978-6855381, behind LMC, and falls in the OGLE field LMC198.69 (Udalski et al. 2008). The well-followed I-band light curve of OGLE-2003-NOOS-005¹² well matches that of SN 1987A. Unfortunately multiband observations for this SN do not exist. The redshift of the host galaxy was spectroscopically determined measuring the positions of a few selected spectral features of a host galaxy spectrum obtained on 2009 August 14 with NTT (equipped with EFOSC2 and grism 11; resolution = 22 \AA). Despite the low signal-to-noise, we identified a few absorption features (Ca II H&K, the g-band $\lambda 4200$, Mg Ib $\lambda 5173$), and H α in emission. In addition the emission line of [O II] $\lambda 3727$ was marginally detected. This allowed to fix the redshift at $z = 0.0302 \pm 0.0008$ ($v_{rec} \approx 9151 \pm 236 \text{ km s}^{-1}$), which corresponds to a distance of about 127 Mpc ($\mu = 35.52$ mag). These values are remarkably similar to those reported by NED ($v_{rec} \approx 9176 \pm 45 \text{ km s}^{-1}$; Jones et al. 2009). and HyperLeda ($v_{rec} \approx 9177 \pm 60 \text{ km s}^{-1}$). The recessional velocity corrected for Local Group infall into the Virgo Cluster is slightly lower ($v_{Vir} \approx 8882 \text{ km s}^{-1}$). Adopting the Hubble Constant value of $H_0 = 72 \text{ km s}^{-1} \text{ Mpc}^{-1}$, we obtain a distance of 123.4 Mpc, i.e. distance modulus $\mu = 35.46$ mag. We also assume in our analysis a total reddening toward the transient of $E(B - V) = 0.16 \pm 0.10$ mag. This was determined including the contribution of the Galaxy $E_{MW}(B - V) = 0.075$ mag (Schlegel et al. 1998) and the reddening at the position of 2MASX J05553978-6855381 due to the intrinsic contribution of LMC that was computed using the maps of Zaritsky et al. (2004) ($E_{LMC}(B - V) = 0.087$ mag). The I-band light curve of this SN is shown in Appendix B.

¹² available via ftp through the OGLE-III (2003 season) web site <http://ogle.astrouw.edu.pl/ogle3/ews/NOOS/2003/noos.html>

8. **SN 2004em** was discovered by Armstrong (2004) on Sept. 14, 2004 when the SN was at $mag = 17.5$. The transient, later classified as a young type II by Filippenko et al. (2004), was hosted in an Sc galaxy (IC 1303). The object was significantly reddened by Galactic dust ($E(B - V) = 0.108$, from Schlegel et al. 1998). Preliminary information on the Caltech Core-Collapse Project light curve has been provided by Gal Yam et al. (2007).
9. **SN 2005ci**, a LOSS discovery (Madison & Li. 2005), was classified as a type II SN by Modjaz et al. (2005) on the basis of the presence of P-Cygni Balmer lines. Its peculiar light curve was first noted by Arcavi et al. (2009), and some early-time unfiltered photometry was provided by Kleiser et al. (2011), showing a clear light curve rise by about 2.5 mag in ~ 45 days. Unfortunately, with the modest amount of data available so far, we cannot estimate the main SN parameters. The host galaxy, NGC 5682, is an Sb-type; the Galaxy reddening is modest, $E(B - V) = 0.033$ mag (Schlegel et al. 1998), but the relatively red continuum shown by the spectrum presented by Kleiser et al. (2011) (see their Figure 12) suggests a non negligible host galaxy reddening. The narrow host galaxy Na ID feature is not clearly detected and the amount of internal reddening cannot be constrained.
10. **SN 2006V** was discovered in the course of the Taiwan Supernova Survey on Feb. 4, 2006 UT at a magnitude of about 18 (Chen et al. 2006). The object was classified as a type II SN after maximum by Blondin et al. (2006) and extensively followed by the Carnegie Supernova Project collaboration, who noted the slowly rising, 1987A-like light curve (Taddia et al. 2011). The galaxy hosting SN 2006V is UGC 6510, which is classified as a face-on spiral (SABc, HyperLeda source) suffering of small Galactic reddening ($E(B - V) = 0.029$ mag, Schlegel et al. 1998). The lack of detection of narrow Na ID absorption at the redshift of UGC 6510, suggest no additional host galaxy extinction toward SN 2006V (Taddia et al. 2011). A comparison between the multi-band light curves of SNe 2006V and 1987A can be found in Figure 3 of Taddia et al. (2011).
11. **SN 2006au** was a discovery of the Tenagra Observatory Supernova Search using the 0.35-m Tenagra telescope in Oslo (on Mar. 7.20 UT). At the discovery, the object had mag 17.2 (Trondal et al. 2006). SN 2006au was later classified by the Nearby Supernova Factory as a type II SN (Blanc et al. 2006). Again, a comprehensive study is presented in Taddia et al. (2011) and comparisons with the light curves of SN 1987A are shown in their Figure 4. The host galaxy, UGC 11057, is a late spiral (possibly an Sc-type, according to HyperLeda) with rather large Galactic reddening, i.e. $E(B - V) = 0.172$ mag (Schlegel et al. 1998). However, Taddia et al. (2011) found that SN 2006au suffered also of large extinction due to dust in the host galaxy, deriving a total reddening of $E(B - V)_{tot} = 0.312$ mag.

tioned in Sect. 4, data for SN 2004em have not been published yet.

Appendix B: Light Curves of 1987A-like events

In this section, the light curves of eight 1987A-like type II SNe are compared with those of the prototype SN 1987A (solid or dashed blue lines, see Figures B.1 and B.2). The light curves of SN 1987A are arbitrarily shifted in magnitude to match the peak magnitudes of the other objects. In the comparison, we assumed the JD s listed in Table 4 as explosion epochs. For a few individual events (e.g. SNe 1982F or 2000cb) the 1987A-likeness is more evident in the red bands than in the blue ones. As men-

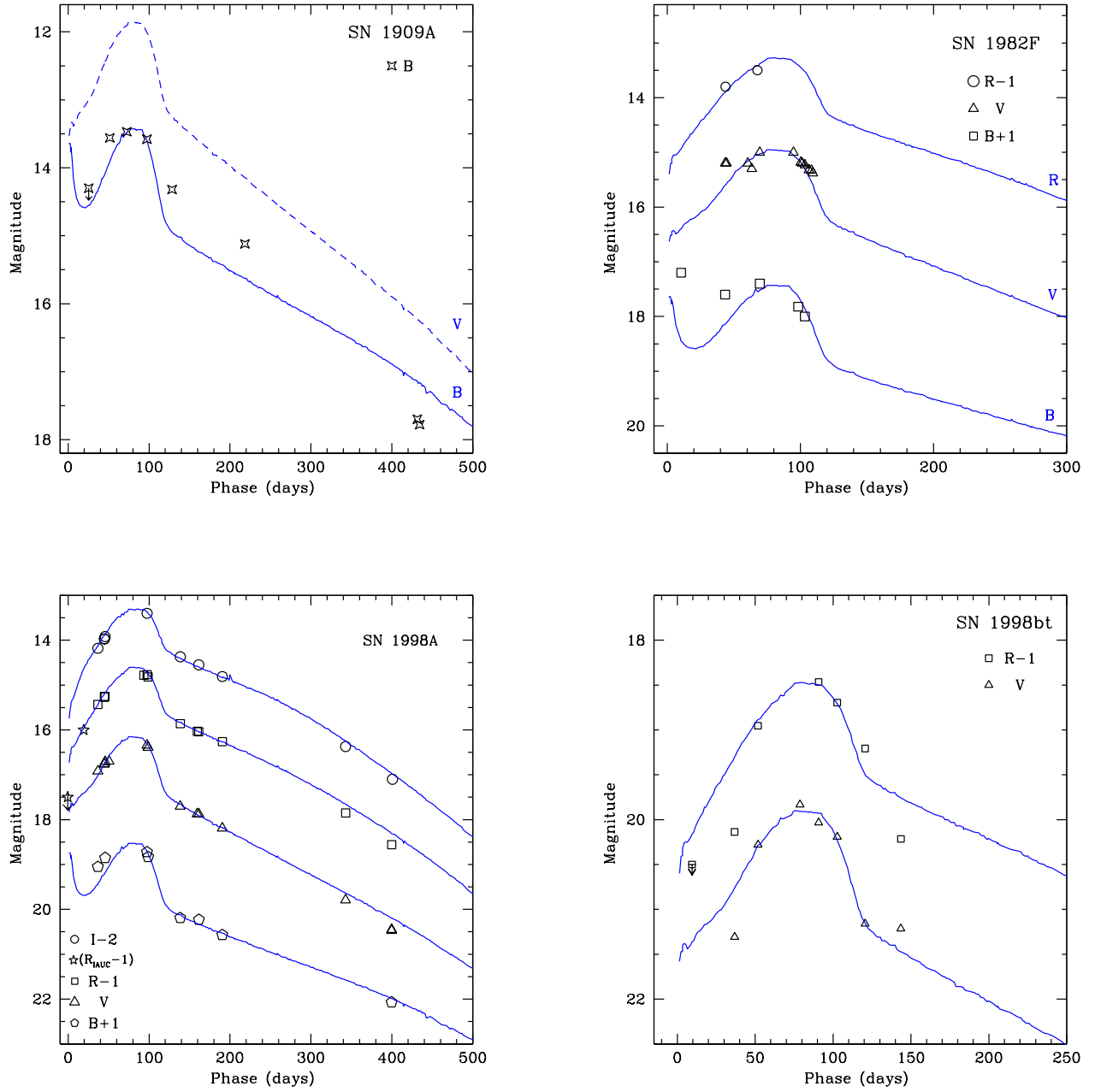


Fig. B.1. Light curves of 1987A-like events: first group of 4 events. The solid (or dashed) blue lines represent the light curves of SN 1987A, our template. The light curves of SN 1987A have been arbitrarily shifted in magnitude to match the peaks of the other transients.

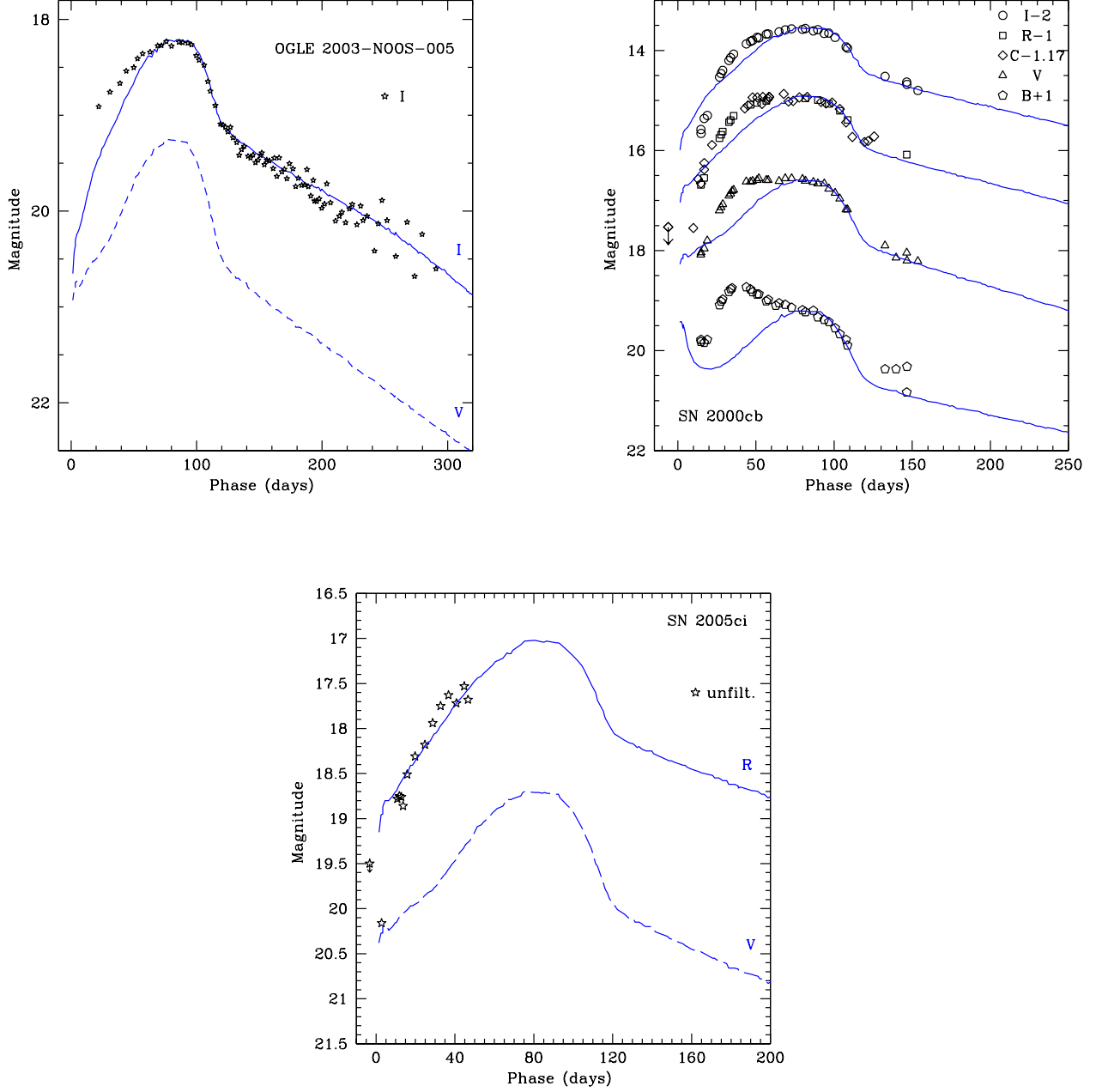


Fig. B.2. Light curves of 1987A-like events: second group of 3 events. The solid (and dashed) blue lines represent the light curves of SN 1987A, our template. The light curves of SN 1987A have been arbitrarily shifted in magnitude to match the peaks of the other transients.